Title

Integration of light and photoperiodic signaling in transcriptional nuclear foci

Eirini Kaiserli [1, 2 *], Katalin Paldi [2], Liz O' Donnell [2], Olga Batalov [1], Ullas V. Pedmale [1], Dmitri A. Nusinow [3, 4], Steve A. Kay [3, 5], Joanne Chory [1*]

[1] Howard Hughes Medical Institute and Plant Biology Laboratory, The Salk Institute for Biological Studies, La Jolla, CA 92037, USA

[2] Institute of Molecular, Cell and Systems Biology, University of Glasgow, Glasgow, G12 8QQ, UK

[3] Center for Chronobiology, University of California, San Diego, La Jolla, CA 92093, USA

[4] Present address: Donald Danforth Plant Science Center, St Louis, MO 63132, USA

[5] Present address: Molecular and Computational Biology Section, University of Southern California, Los Angeles, CA 90089, USA

* **Correspondence**: eirini.kaiserli@glasgow.ac.uk and chory@salk.edu

Running title

TZP induces flowering in transcriptional foci

Summary

Light regulates major plant developmental transitions by orchestrating a series of nuclear events. This study uncovers the molecular function of the natural variant, TZP (Tandem Zinc-finger-Plus3), as a novel signal integrator of light and photoperiodic pathways in

transcriptional nuclear foci. We report that TZP acts as a positive regulator of photoperiodic flowering via physical interactions with the red-light receptor phytochrome B (phyB). We demonstrate that TZP localizes in dynamic nuclear domains regulated by light quality and photoperiod. This study shows that phyB is indispensible not only for localizing TZP to transcriptionally active nuclear photobodies, but also for recruiting TZP on the promoter of the floral inducer *FLOWERING LOCUS T (FT).* Our findings signify a unique transcriptional regulatory role to the highly enigmatic plant nuclear photobodies, where TZP directly activates *FT* gene expression and promotes flowering.

Introduction

Light, circadian rhythms and hormones act as informational cues for optimizing plant development in response to the constantly changing environment. Genetic analysis in *Arabidopsis* has been instrumental for identifying key players involved in fundamental developmental transitions such as de-etiolation and flowering. In particular, the blue-light receptors cryptochrome 2 (cry2), FLAVIN-BINDING, KELCH REPEAT, F-BOX 1 (FKF1), the red-light receptors phytochrome A (phyA) and phyB regulate the abundance and activity of transcription factors (TFs) such as CONSTANS (CO) and PHYTOCHROME INTERACTING FACTORS (PIFs) (Andres and Coupland, 2012; Leivar and Quail, 2011). The majority of the molecular and cellular events triggering flowering and photomorphogenesis are regulated by light and clock signal transduction pathways that collectively induce changes in gene expression (Cerdan and Chory, 2003; Song et al., 2012b; Tepperman et al., 2001; Wigge et al., 2005). The mechanism and site where photosensory pathways and transcriptional machineries integrate to modulate plant

responses and optimize growth still remains enigmatic. As a means of achieving signal integration, many light and clock signaling components converge in the nucleus and form microdomains, also known as photobodies (Chen et al., 2010; Van Buskirk et al., 2012; Van Buskirk et al., 2014). However, the exact location, molecular function(s), mode of assembly, composition and physiological significance of nuclear photobodies remain to be uncovered. In addition to protein interactions, a series of highly dynamic nuclear events such as chromatin reorganization and gene relocation have been observed to occur prior to global changes in gene expression during de-etiolation and flowering initiation (Feng et al., 2014; van Zanten et al., 2012). How environmental and endogenous stimuli integrate at the level of gene expression and which of these signaling components are essential for orchestrating nuclear organization is still unknown. In higher eukaryotes transcriptional machinery, active gene loci and chromatin remodeling enzymes have been shown to compartmentalize in punctate nuclear foci (Papantonis and Cook, 2013; Sutherland and Bickmore, 2009). Elegant studies have demonstrated the re-positioning of light regulated genes to the nuclear periphery of *Arabidopsis* cells, however, the existence and composition of transcriptional foci and the possibility of active gene regions moving towards areas enriched in transcriptional regulators remains to be elucidated in plants (Feng et al., 2014).

Natural genetic diversity provides a great source of information for identifying novel, physiologically significant transcriptional regulators with fundamental roles in fine-tuning plant growth and survival. In this study we focus on characterizing a new nuclear signal integrator identified as the causative locus regulating morning-specific growth by Quantitative Trait Locus (QTL) mapping between the natural *Arabidopsis* ecotypes Bay-0

and Shahdara (Loudet et al., 2008). Tandem Zinc-finger Plus3 (TZP) is a single copy gene that encodes a unique nuclear protein in *Arabidopsis* containing a combination of Zinc Finger (ZF) and PLUS3 domains. ZF domains act as interaction sites for RNA, DNA or proteins (Ciftci-Yilmaz and Mittler, 2008) and are commonly found in transcriptional regulators in combination with other DNA-binding motifs (Hu et al., 2008). PLUS3 domains are also involved in nucleotide binding, but possess higher affinity for RNA and single-stranded DNA (de Jong et al., 2008). Studies in yeast and human proteins have revealed that PLUS3 domains function in chromatin re-organization by mediating the recruitment of gene regulatory proteins and RNA-processing factors to chromatin during transcription (Wier et al., 2013). However, the function of PLUS3 domains in plant species has not yet been studied. Microarray analysis on *Arabidopsis* seedlings showed that TZP controls a number of genes ranging from photoreceptors to transcription factors, growth regulators and chromatin remodeling factors (Loudet et al., 2008). Furthermore, promoter analysis of TZP-regulated genes show over-representation of the HUD (Hormone Up at Dawn) cis-acting element, which has previously been associated with growth promoting genes that respond to light and hormones at dawn (Michael et al., 2008). These initial studies indicate that TZP is a key transcriptional regulator of plant growth processes in response to environmental and endogenous stimuli. However, information on the mode of TZP action, its interacting partners and nuclear dynamics is currently lacking. This study not only characterizes the molecular function and protein interactions of TZP in nuclear photobodies, but it also identifies a direct role in regulating photoperiodic flowering at the transcriptional level.

Results

TZP localizes in dynamic nuclear photobodies

To characterize the mechanism of TZP action in regulating gene expression we employed cytogenetic, biochemical and molecular approaches. Transgenic *Arabidopsis* plants expressing TZP fused to fluorescent markers (GFP, YFP, mCitrine or mCherry) driven by either the native or constitutive promoters showed that TZP is exclusively localized in the nucleus and forms highly dynamic nuclear foci in light-grown plants (Figure S1A). Formation of such sub-nuclear structures is independent of protein accumulation indicating that TZP nuclear bodies (NB) have functional significance rather than being artefacts of overexpression. The presence of photoreceptors and major light signaling components in nuclear photobodies is well documented (Van Buskirk et al., 2012). TZP has been previously shown to regulate photomorphogenesis and hypocotyl elongation (Loudet et al., 2008). To test if the formation on TZP nuclear bodies is induced by specific wavelengths of light, etiolated seedlings expressing *35S*$_{pro}$TZP-GFP were irradiated with blue, red, far-red and white light (Figure 1A). Confocal image analysis showed that irradiation of etiolated seedlings with red light triggers rapid formation (within 10 s) of multiple TZP-GFP nuclear bodies (Figure 1A). Whereas TZP-GFP is uniformly localized in the nucleoplasm when plants are kept in dark or exposed to blue or far-red light (Figure 1A). Coilin-RFP was used as a control protein that forms constitutive nuclear bodies independent to light quality or fluence rate (Figure 1A) (Collier et al., 2006). Western blot analysis shows that light treatments that induce NB formation do not affect TZP-GFP or coilin-RFP protein levels (Figures 1B and S1B). These observations suggest that TZP NB formation does not affect TZP protein stability. To investigate the diurnal and circadian regulation of TZP nuclear

body formation, plants entrained to light/dark cycles were examined. To quantify this response, the average number of nuclear bodies per nucleus was plotted for each time-point and light condition examined (Figure 1C). Minimal nuclear body formation was observed during the night and maximal during the day. The same oscillating pattern was present when plants entrained to a light/dark cycle were kept in darkness for up to 24 hours. To define the wavelength specificity of the diurnal regulation of TZP nuclear body formation, plants were entrained under a blue-light/dark or red-light/dark cycle. High amplitude oscillations were observed in red light (Figure 1C). A similar pattern has previously been reported for the nucleo-cytoplasmic partitioning and nuclear body formation of phytochromes (Kircher et al., 2002). No significant changes in TZP-GFP and endogenous TZP protein levels were observed in response to a light/dark photoperiod (Figure S1C).

To investigate the dynamics and mobility of TZP-GFP we performed Fluorescence Recovery After Photobleaching (FRAP) experiments on single nuclear bodies, nucleoplasmic areas or whole nuclei (Figure 2). The recovery of TZP-GFP fluorescence in nuclear foci occurs within seconds, whereas nucleoplasmic TZP-GFP fluorescence recovers much slower (Figure 2A-B). Measurements were normalized by monitoring the fluorescence changes due to imaging of non-bleach areas within the same nucleus. Control FRAP on whole nuclei showed no recovery within the time-period examined suggesting that new TZP protein would need to be synthesized and transported into the nucleus, which would require longer periods of time exceeding the timescale of the FRAP experiment (Figure 2C). These data indicate that there is rapid exchange between the nucleoplasmic and NB TZP pools and an active recruitment of TZP protein into nuclear

microdomains, which is highly consistent with previous observations on phyA nuclear dynamics (Rausenberger et al., 2011).

TZP interacts, co-purifies and co-localizes with phyB in nuclear photobodies

In order to assign a function to TZP nuclear photobodies we performed co-localization studies with proteins of known function that concentrate in nuclear microdomains. PhyB is one of the best-characterized light signaling components that concentrates into nuclear foci in a photo-dynamic manner (Kircher et al., 1999; Yamaguchi et al., 1999). To assess if TZP occupies the same nuclear photobodies as phyB we performed co-localization studies between TZP-mCherry and phyB-CFP. Transient expression assays in *Nicotiana benthamiana* show that TZP and phyB co-localize in nuclear bodies in white light (Figure 3A). In addition to phyB, TZP co-localizes with the scaffold protein EARLY FLOWERING 3 (ELF3) known to modulate flowering and hypocotyl growth in response to light and the circadian clock (Figure 3A) (Nusinow et al., 2011; Yu et al., 2008). Partial overlap in localization was observed between TZP and PIF4 in very small but not in large nuclear photobodies, whereas TZP and HEMERA (HMR) co-localized only in the nucleoplasm (Figure S2B). Phytochrome NBs act as sites for PIF and phyA degradation during the initial stages of photomorphogenesis (Al-Sady et al., 2006; Bauer et al., 2004; Chen et al., 2010; Seo et al., 2004). HMR is involved in the degradation of phyA and PIF TFs (Qiu et al., 2015). On the contrary, the localization of TZP in NBs does not affect its protein stability (Figure 1B) suggesting that TZP-phyB NBs may have a distinct function compared to the nuclear sites of PIF degradation, whereas the extremely small TZP-PIF4 NBs could have a

storage role similar to the one described for small phyB NBs during shade avoidance response at later developmental stages (Trupkin et al., 2014).

We next, examined whether TZP co-localizes with nuclear body components of known function such as coilin (Cajal body component), fibrillarin (nucleolar pre-rRNA splicing) or U2B (spliceosomal coiled bodies) (Boudonck et al., 1999; Collier et al., 2006; Koroleva et al., 2009). However, no detectable co-localization signal was observed between TZP and coilin, fibrillarin or U2B (Figure S2A) indicating that TZP resides in specialized nuclear domains formed in response to red light and contain light and clock signaling components.

In addition to co-localization studies, a direct interaction between TZP and PHYB apoprotein was confirmed using the yeast-two-hybrid interaction assay (Figure 3B). Quantitative interaction studies show that the N-terminus of TZP is sufficient for protein association with the PHYB apoprotein in yeast in the absence of phytochromobilin (Figure 3B). No physical interaction was observed between TZP and PHYA apoprotein. Bait and prey constructs were assessed for auto-activation to eliminate false positive interactions on selective media and by performing a quantitative X-gal assay (Figure S2C-D). To complement the co-localization and yeast-two-hybrid analysis, we tested if TZP associates with phyB in transgenic *Arabidopsis* lines expressing TZP-GFP by co-immunoprecipitation assays. Figure 3C shows that TZP-GFP co-precipitates native phyB primarily in response to red light. Plants not expressing TZP-GFP, or plants expressing a nuclear TF tagged with GFP used as negative controls did not show co-purification with phyB (Figure S2E). Collectively, our data show that TZP and phyB interact directly *in vivo* and *in vitro* and that TZP is recruited to phyB-enriched nuclear photobodies in response to red light.

PhyB is indispensible for recruiting TZP in photobodies

To understand the mechanism and biological significance of TZP recruitment in nuclear domains, we examined the localization pattern of TZP in the absence of functional phytochromes. PhyB localization in NBs is red light-dependent, while the N-terminus of phyA is sufficient to localize in NB in response to red, far red and blue light, therefore we determined if phyB or phyA were necessary for TZP localization to NBs (Viczian et al., 2012) (Figure 3D). Transgenic *Arabidopsis* lines expressing TZP-GFP in the *phyB* mutant background show a lack of nuclear body formation in response to red light (Figure 3D). On the contrary, phyA is not required for TZP nuclear body formation, suggesting that TZP is recruited to photobodies independently of phyA (Figure 3D) consistent with the lack of direct interaction between PHYA apoprotein and TZP in yeast (Figure 3B). These data highlight the specificity of TZP-phyB interaction and the role of phyB in recruiting TZP in nuclear domains.

Nuclear photobodies are sites of active transcription

To discover a potential role and biological significance of TZP association in nuclear photobodies, we examined the effect of pharmacological inhibitors on NB formation. More specifically, we investigated the effect of inhibitors of RNA polymerase [α-amanitin, 5,6-Dichloro-1-β-D-ribofuranosylbenzimidazole (DRB)], DNA-primed RNA synthesis (actinomycin D) or protein kinases (staurosporine). TZP NBs were completely disrupted following treatments with α-amanitin, DRB and actinomycin D, all of which are known to block transcription. In particular, actinomycin D and DRB resulted in the formation of one

large TZP nuclear aggregate, in accordance with previous studies in mammalian cells demonstrating enlargement of speckles (Lamond and Spector, 2003). The localization pattern of coilin-RFP remained unchanged suggesting that the pharmacological treatments had no aberrant effects on global nuclear organization (Figure 4A) (Koroleva et al., 2009). No effect was observed when plants expressing TZP-YFP or coilin-RFP were incubated with control solvent DMSO or the kinase inhibitor staurosporine (Figure S3B). Western blot analysis determined that mislocalization of nuclear TZP was independent of changes in TZP protein levels (Figure S3A). A similar pattern was observed when phyB-CFP was treated with α-amanitin but not in plants treated with control DMSO solution (Figure 4A).

Furthermore, to examine the presence of nucleic acids in TZP nuclear bodies, heterochromatin markers (DAPI) and an RNA selective probe, E144, were used for co-localization studies with TZP-YFP (Li et al., 2006; van Zanten et al., 2012). TZP nuclear photobodies co-localize with the RNA selective probe E144 but not with DAPI (Figure 4B). In plants, DAPI stains chromocentres and highly compacted chromatin regions with limited transcriptional activity (van Zanten et al., 2012).

PLUS3 domains of yeast and human RTF1 interact with single-stranded but not double-stranded DNA in vitro (de Jong et al., 2008), (Wier et al., 2013). To assess if TZP PLUS3 domain has a similar role in plants, we performed *in vitro* DNA binding assays. Equal amounts of epitope-tagged TZP, $TZP^{ZFPLUS3}$, TZP^{PLUS3}, TZP^{ZF1+2} or the TF ATHB23 were incubated with single-stranded or double-stranded DNA as previously described for HUA proteins (Li et al., 2001) (Figure S3C) (Figure 4C). TZP protein deletion analysis clearly demonstrates that the PLUS3 domain of TZP is necessary and sufficient for binding specifically to single-stranded but not double-stranded DNA (Figure 4C), similar to the

PLUS3 domain from yeast Rtf1. The Zinc-Finger Homeobox domain TF, ATHB23, was used as a positive control for the assay showing binding to both ss and dsDNA (Figure 4C) (Tan and Irish, 2006). Although $TZP^{ZFPLUS3}$ is necessary for conferring binding to ssDNA, it is not sufficient for NB formation when expressed in WT, Bay-0 or transiently in N. *benthamiana* (Figure S3D) indicating that the recruitment in nuclear photobodies is highly specific and requires the fully functional TZP protein.

Collectively, our data indicate that the nuclear microdomains formed by TZP and concomitantly phyB are associated with active gene expression, transcriptional initiation or co-transcriptional RNA processing similar to the mechanism described for Rtf1, a component of the yeast and human Polymerase Associated Factor (PAF) complex (de Jong et al., 2008; Wier et al., 2013).

TZP promotes flowering

To determine the physiological significance of the interaction between phyB and TZP, two predominant light responses were examined: hypocotyl elongation and flowering time. Although we employed multiple approaches to generate *tzp* knockout and knock down mutant lines, we were unsuccessful. Bay-0 contains a non-functional TZP variant due to a pre-mature stop codon within its PLUS3 domain (Loudet et al., 2008). Therefore we used an alternative approach and overexpressed TZP (TZP WT) in WT and Bay-0 to characterize the function of TZP protein in *Arabidopsis*. More specifically, we measured hypocotyl elongation and flowering time phenotypes in excess of functional TZP (Figure S4A) in response to different light wavelengths, photoreceptor and light signaling mutant backgrounds. The role of phyB and the blue light receptor cry2 are well established in

regulating flowering time and hypocotyl elongation (Cerdan and Chory, 2003; Guo et al., 1998; Neff and Chory, 1998). Transgenic plants expressing *35S*$_{pro}$TZP-GFP showed no significant changes with respect to the inhibition of hypocotyl growth in response to red or far-red light, a response primarily controlled by the phytochromes (Figure S4A). However, in accordance with the data published previously, TZP promotes hypocotyl elongation in response to blue light (Figure S4A) (Loudet et al., 2008).

Since TZP associates with phyB and regulates the expression of photoperiodic and clock controlled morning-specific genes containing the HUD promoter element (Loudet et al., 2008), its role in regulating flowering time was examined. Overexpression of TZP in wild type (WT) or Bay-0 leads to early flowering when plants are grown under long day (Figure 5A and S4B), but not under short day photoperiodic conditions (Figure S4D). To exclude the possibility that TZP induces flowering due to a non-specific pathway, we showed that the transcript levels of the stress-responsive gene *ERD10* that plays a role in the control of flowering in response to abiotic stress remained unchanged in TZP WT and TZP Bay-0 lines (Figure S4E) (Corrales et al., 2014). Relatively earlier flowering time was also observed when TZP was overexpressed in the extremely delayed flowering mutant *cry1cry2* (TZP *c1c2*), whereas there was no difference when TZP was overexpressed in the early flowering *phyB* mutant (TZP *phyB*) (Figure 5A and 7A). These data suggest that TZP is a positive regulator of flowering via a phyB-dependent signal transduction pathway.

TZP regulates *FT* expression via chromatin association

In *Arabidopsis*, long day photoperiods induce flowering via the action of the floral inducer FT (Kardailsky et al., 1999). Environmental and endogenous stimuli integrate at the level of

transcriptional regulation of *FT* (Song et al., 2012a). Therefore, we examined *FT* transcript levels in multiple transgenic lines overexpressing TZP. Indeed, overexpression of TZP in WT and Bay-0 (TZP Bay) leads to an increase in *FT* transcript abundance (Figure 5C and S4C). Quantitative RT-PCR analysis shows that TZP WT induces both *FT* and *CO* transcript abundance in plants grown for 12 days under LD photoperiod but not in 4-day old seedlings (Figure 5B and S5B). To examine why *FT* was not previously identified in microarray studies performed on 4-day old seedlings as one of the target genes up-regulated by TZP (Loudet et al., 2008), we performed qRT-PCR on 12 and 4-day old seedlings overexpressing TZP under long day photoperiodic conditions in white, blue or red light and showed that TZP induces *FT* expression in 12 day but not 4-day old plants (Figure 5B). These data signify a developmentally specific function for TZP after the initial stages of photomorphogenesis and de-etiolation. CO protein is known to accumulate at dawn (ZT0.5) and subsequently targeted for degradation by ZT4 in a phyB-dependent manner, whereas at the end of the day (ZT15) phyA and cry2 stabilize CO that induces *FT* expression (Valverde et al., 2004). Our data show that phyB is necessary for the increase in the induction of *FT* and *CO* gene expression observed in TZP WT plants at midday (ZT8) and dawn (ZT0.5) as TZP *phyB* lines show impaired *FT* and *CO* mRNA accumulation (Figure 5C, S4F-G and S5B). The magnitude of TZP-mediated *FT* and *CO* induction is greatly increased at ZT15 even in *phyB* mutant plants that already show higher *FT* expression due to the lack of CO degradation (Figure S4G and S4G). These data would suggest that at dusk TZP enhances the induction of *FT* and *CO* expression through the synergistic action of clock components, photoreceptors and transcriptional regulators

such as phyA, cry2, FKF1, TOE1 or PFT1 (Cerdan and Chory, 2003; Sawa et al., 2007; Valverde et al., 2004; Zhang et al., 2015).

A direct role of TZP in regulating *FT* gene expression was examined by Chromatin Immunoprecipitation (ChIP) assays, using transgenic lines expressing GFP-tagged TZP. TZP-specific enrichment was detected in amplicons III, IV, and V, which are adjacent to the *FT* transcriptional start site (TSS) (Figure 6A). No TZP enrichment was observed on $HY5^{pro}$, which is a light-regulated gene unaffected by TZP (Figures 6A and S5A). Homozygous transgenic lines overexpressing equal protein levels of TZP deletion variants (TZP^{Nt}, $TZP^{ZFPLUS3}$) show that the full-length TZP protein is essential for association to FT^{pro} and induction of *FT* gene expression (Figures 6B-C and S5D), which is consistent with the localization studies showing that $TZP^{ZFPLUS3}$ is not sufficient for NB formation (Figure S3D). As previously mentioned, the N-terminus of TZP is required for interaction with the PHYB apoprotein (Figure 3B). Therefore the N-terminus and ZF domains of TZP may provide a platform for protein interactions that activate a regulatory mechanism for sequence-specific binding upon stimulus activation *in planta*. Furthermore, the fact that the overexpression of TZP deletion variants cannot induce *FT* expression supports our model that the early flowering phenotype observed in TZP WT and TZP Bay-0 is not due to a dominant negative effect of overexpression.

Transgenic lines overexpressing TZP in the *phyB* mutant showed no enrichment on FT^{pro} or CO^{pro} (Figures 6D and S5C). Further evidence supporting phyB-dependent enrichment of TZP on FT^{pro} is demonstrated by the far-red light reversibility (Figure 6E). No significant enrichment was detected for phyB-CFP on either *FT* or *HY5* promoters (Figure S5E). These data suggest that phyB may associate transiently with the transcriptional

machinery. Therefore, more potent cross-linking reagents may be required in order to capture a putative residency of phyB on regulated loci. TZP-GFP is able to associate with FT^{pro} and up-regulate *FT* expression when overexpressed in *cry1cry2* (Figures 7B and S6). Western blot analysis shows that this is not due to lower TZP-GFP protein levels when expressed in *phyB* compared to WT or *cry1cry2* genotypes (Figure 7C). These data indicate that TZP controls FT-mediated flowering through a phyB-dependent pathway.

Discussion

Previous studies using QTL mapping have identified TZP as a novel signaling component regulating plant growth at the level of gene expression (Loudet et al., 2008). In addition to the role of TZP in blue light induced hypocotyl elongation during de-etiolation, we have uncovered a new role for TZP in regulating flowering initiation. Blue and red light signal transduction pathways are known to act synergistically as well as antagonistically in regulating photomorphogenesis (Hughes et al., 2012; Mas et al., 2000; Sellaro et al., 2009). Therefore, it is possible that TZP has distinct roles in regulating blue light dependent hypocotyl growth during early photomorphogenesis and flower initiation that may depend on the tissue and interactome context at different developmental stages.

The biogenesis, function and composition of nuclear photobodies have remained a mystery since their discovery over ten years ago. Our results support the hypothesis that nuclear photobodies have an active role in regulation of gene expression. More specifically, we have identified phyB as the interacting photoreceptor that recruits TZP in nuclear microdomains (Figure 3). Recent studies using a nucleolus tethering system suggest that the majority of light signaling components follow a self-organization model to form nuclear

micro-domains or photobodies (Liu et al., 2014; Matera et al., 2009). Pharmacological and cytogenetic studies indicate that TZP-phyB nuclear photobodies act as regulatory sites of gene expression at the level of transcription (Figure 4). The idea of concentrating transcriptional machinery and active chromatin regions within localized nuclear domains is an established concept in higher eukaryotic systems (Papantonis and Cook, 2013; Sutherland and Bickmore, 2009). However, the existence and composition of transcriptional foci in *Arabidopsis* and other plant species is open to investigation. Our data support the hypothesis that nuclear photobodies have a direct role in actively regulating gene expression at the level of transcription in plants. Collectively, these findings assign a functional role to the recruitment of signaling components in nuclear photobodies. Our data are in accordance with recent studies showing that phyB plays a role in inducing alternative splicing and transcription simultaneously (Shikata et al., 2014). TZP is one of the very few proteins in *Arabidopsis* containing the highly conserved PLUS3 domain known to facilitate transcriptional elongation by recruiting transcriptional machinery, chromatin remodeling and splicing factors in yeast and humans (Ciftci-Yilmaz and Mittler, 2008; de Jong et al., 2008; Wier et al., 2013). Our data indicate functional conservation between the PLUS3 domain of Rtf1 and TZP with respect to ssDNA binding. It would be very important to assess the role of TZP in transcriptional elongation and co-transcriptional splicing, especially since phyB has an active role in regulating alternative splicing processes in *Arabidopsis* (Shikata et al., 2014).

In this study we have uncovered the molecular mechanism of TZP function as a transcriptional integrator of red light and photoperiodic signaling pathways regulating flowering. We find that overexpression of TZP accelerates flowering due to a TZP-induced

increase in *FT* and *CO* transcript abundance (Figure 5 and S5B). We dissected the mechanism of activation of *FT* gene expression by performing ChIP qPCR in different mutant backgrounds and we show that TZP can associate with the promoter of *FT* and *CO*. Moreover, phyB is essential not only for TZP nuclear body formation, but also for the association of TZP on FT^{pro} and CO^{pro} and consequently for the induction of *FT* and *CO* expression (Figure 3D, 5, 6 and S5C). The majority of proteins acting downstream of phyB regulate de-etiolation or shade avoidance responses (Castillon et al., 2007). PhyB is known to indirectly negatively regulate *FT* expression by promoting CO degradation in a morning specific manner (Valverde et al., 2004). Previous studies have reported genetic interactions between phyB and cryptochromes as a means of mediating cross-talk between the red/far-red and blue light signaling to fine-tune plant development in response to diverse spectral inputs (Hughes et al., 2012; Mas et al., 2000; Sellaro et al., 2009). PhyB and cry2 have been shown to control reversible chromatin compaction in response to different light regimes (van Zanten et al., 2010). However, our studies show that TZP acts independent of cryptochromes to regulate flowering time (Figure 6). This study has uncoupled the role of TZP from blue light mediated photomorphogenesis and assigned a novel function to TZP in regulating flowering via red light mediated transcriptional regulation. Our findings indicate that TZP operates through a blue light specific pathway during the early stages of de-etiolation, whereas it associates with red light and clock signaling components to regulate the transition from vegetative to reproductive growth during later stages of plant development. Furthermore, our data provide evidence for a novel, phyB-mediated pathway that directly regulates *FT* expression via TZP recruitment to its promoter. The TZP-dependent pathway is more likely to be synergistic or additive to the

CO-dependent pathway and antagonistic to phyB-mediated CO protein degradation (Figure 7D). qRT-PCR analysis show negligible TZP-dependent induction of *FT* and *CO* in the absence of phyB at ZT0.5 and ZT8 (Figure 5B and S4F-G) suggesting that TZP acts through a phyB dependent pathway in a diurnal specific manner. The fact that in the absence of phyB TZP cannot associate with FT^{pro} or CO^{pro} and therefore cannot up-regulate *FT* or *CO* transcript levels also argues against but does not exclude the possibility that TZP indirectly promotes flowering by rescuing CO from phyB-dependent degradation, as demonstrated by Phytochrome-dependent Late-flowering (PHL) association and phyB overexpression (Endo et al., 2013; Hajdu et al., 2015). Our model suggests that TZP acts as a positive regulator of photoperiodic flowering by inducing the expression of *FT* and *CO*. The action of TZP is tightly regulated by phyB, which could potentially operate as a gate-keeper establishing a balance between *FT, CO* transcript abundance and CO degradation. Overexpression of TZP leads to an increase in the overall amplitude of *FT* and *CO* gene expression during the day, therefore tilting the balance towards the positive regulatory role of phyB. A potential physiological role of the native TZP protein and phyB interaction is to maintain a basal pool of *CO* and *FT* mRNA levels that primes CO protein stabilization as a means of enhancing the induction of flowering. To dissect the relationship between the CO and TZP-dependent pathways it would be essential to analyze *tzp* knockout and *co* mutant lines overexpressing TZP.

TZP represents a great example where natural variation has engineered the function of a single signaling component to fine-tune photomorphogenesis and flowering time in response to changes in light and photoperiod. This study opens new avenues in investigating the molecular function of nuclear photobodies as integrating hubs of major

signaling components that form in response to environmental and endogenous stimuli to regulate gene expression and optimize plant growth. Furthermore the physical interaction between TZP and phyB provide an excellent system for studying the formation, composition, molecular function and physiological role of transcriptionally active photobodies as hubs of signal integration.

Experimental Procedures

Protein extraction, protein and chromatin immunoprecipitation assays

ChIP assays were performed on plants grown under a long day photoperiod (16L/8D) and tissue was cross-linked at ZT8 as described previously prior to freezing in liquid nitrogen unless otherwise stated (Brown et al., 2005). Protein extraction was performed as described previously (Nusinow et al., 2011). One mg of total protein was used for co-immunoprecipitation assays using the μMACS^{TM} GFP Tag Protein Isolation Kit. Denaturing elution was performed according to the manufacturer's instructions (Miltenyi Biotech).

Pharmacological treatments

Inhibitor and control treatments were performed on 4-day old seedlings and mature plant leaf tissue at concentrations previously determined (Ali and Reddy, 2006; Koroleva et al., 2009; Koroleva et al., 2004) for 2 hours prior to confocal imaging. Western blot analysis was performed on plants that received the same inhibitor treatment as for confocal imaging to determine the effect on protein stability. For all treatments, coilin-RFP (Koroleva et al., 2009) was used as a control.

Confocal microscopy

Confocal microscopy was performed with a Leica SP2, a Zeiss 710 and a Zeiss 510 inverted microscopes and image analysis was performed as described previously (Jaillais et al., 2011; Kaiserli and Jenkins, 2007). FRAP experiments were performed using a Zeiss 710 inverted microscope and images were collected and analysed as described previously (Ali and Reddy, 2006; Kaiserli et al., 2009). Representative images from three independent biological repeats are shown in this study. For quantitative studies the number of nuclear bodies per nucleus of a minimum of 50 cells, 10 independent plants, 3 independent biological repeats was counted. Transient expression and imaging in *N. benthamiana* was performed as described previously (Kaiserli et al., 2009).

DNA binding assay

Full length TZP, TZP deletion variants and ATHB23 proteins fused to a FLAG tag were expressed from an SP6 promoter using the TnT *in vitro* transcription/translation system (Promega®). Equal amounts of protein were incubated with either single-stranded or double-stranded deoxyribonucleic acid lyophilized powder attached to cellulose from calf thymus DNA (0.75 µg/µl) (Sigma) as described previously (Li et al., 2001). After incubation at 4°C for 10 min, the beads were washed five times in RHPA buffer (10 mM Tris,pH 7.4, 2.5 mM $MgCl_2$, 0.5% Triton X-100) and then boiled in SDS loading buffer. The proteins were detected by western blot using an anti-FLAG (Sigma A8592).

RNA extraction and quantitative real-time PCR

Plants were grown under a long day photoperiod (16L/8D) and tissue was harvested at ZT8 by freezing in liquid nitrogen. RNA was extracted using the RNeasy plant mini kit (Qiagen) according to the manufacturer's instructions. 2 µg RNA was used for cDNA synthesis (Superscript II First Strand Synthesis System, Life Technologies) according to the manufacturer's instructions. For each sample 10 µl of 100-fold diluted cDNA sample were used for quantitative real-time PCR using SYBR Select Mastermix (Applied Biosystems, Life Technologies) on a StepOnePlus™ Real-Time PCR System (Applied Biosystems, Life Technologies) according to the manufacturer's instructions. Data shown are representative of three independent biological repeats and four technical replicates.

Additional Methods

Additional information on plant material and growth conditions, DNA constructs, yeast-two-hybrid assays, qRT-PCR analysis, hypocotyl measurements and a list of the primers used are provided in the Supplemental Experimental Procedures.

Author Contributions

E.K., D.A.N., S.A.K. and J.C. directed the research and designed the experiments. E.K. generated DNA constructs, transgenic lines, performed and analysed the data obtained from confocal microscopy, yeast-two-hybrid, immunoblot, ChIP, co-immunoprecipitation, DNA binding and hypocotyl assays. E.K. and D.A.N. co-performed the initial TZP-phyB co-immunoprecipitation assays. K.P. performed and analysed qRT-PCR and ChIP qPCR experiments. O.B. performed the immunoblots of TZP and coilin and L. O' D. the flowering

time experiments. U.V.P. made constructs for *in vitro* assays. All authors commented on the manuscript.

Acknowledgements

We are grateful to Dr. James Fitzpatrick, (Salk Institute) for advice on FRAP measurements and to Dr. Yvon Jaillais (Lyon) for providing plasmids containing $35S_{pro}$, $UBI10_{pro}$, mCITRINE and mCHERRY. We are grateful to Prof. Peter Shaw (JIC) for the gift of coilin-RFP, Prof. Akira Nagatani (Tokyo) for his gift of anti-PHYB antibody and Prof. Young-Tae Chang (Singapore) for the RNA selective probes. Many thanks to Prof. Ferenc Nagy (Edinburgh) and Prof. Eberhard Schäfer (Freiburg) for sharing data and helpful discussions, Dr. Lucio Conti (Milan), Dr. Doris Lucyshyn (Vienna) for advice on flowering experiments and Dr. Stuart Sullivan (Glasgow) for providing the *ISU* primers. We thank Prof. John Christie and Dr. Stuart Sullivan for critically reading the manuscript. The early stages of this work were supported by the NIH grant R01-GM52413 and the Howard Hughes Medical Institute (to J.C.). J.C. is an investigator of HHMI. E.K. was supported by fellowships from the Human Frontier Science Program, the Salk Institute (Pioneer Fund, Kirby and Stern Foundation) and the University of Glasgow (Lord Kelvin and Adam Smith Fellowship). D.A.N. and S.A.K. acknowledge support from the National Institutes of Health (NRSA GM083585 to D.A.N., and R01 GM050006 and GM067837 to S.A.K.).

References

Al-Sady, B., Ni, W., Kircher, S., Schafer, E., and Quail, P.H. (2006). Photoactivated phytochrome induces rapid PIF3 phosphorylation prior to proteasome-mediated degradation. Molecular cell *23*, 439-446.

Ali, G.S., and Reddy, A.S. (2006). ATP, phosphorylation and transcription regulate the mobility of plant splicing factors. Journal of cell science *119*, 3527-3538.

Andres, F., and Coupland, G. (2012). The genetic basis of flowering responses to seasonal cues. Nature reviews. Genetics *13*, 627-639.

Bauer, D., Viczian, A., Kircher, S., Nobis, T., Nitschke, R., Kunkel, T., Panigrahi, K.C., Adam, E., Fejes, E., Schafer, E.*, et al.* (2004). Constitutive photomorphogenesis 1 and multiple photoreceptors control degradation of phytochrome interacting factor 3, a transcription factor required for light signaling in Arabidopsis. The Plant cell *16*, 1433-1445.

Boudonck, K., Dolan, L., and Shaw, P.J. (1999). The movement of coiled bodies visualized in living plant cells by the green fluorescent protein. Molecular biology of the cell *10*, 2297-2307.

Brown, B.A., Cloix, C., Jiang, G.H., Kaiserli, E., Herzyk, P., Kliebenstein, D.J., and Jenkins, G.I. (2005). A UV-B-specific signaling component orchestrates plant UV protection. Proceedings of the National Academy of Sciences of the United States of America *102*, 18225-18230.

Castillon, A., Shen, H., and Huq, E. (2007). Phytochrome Interacting Factors: central players in phytochrome-mediated light signaling networks. Trends in plant science *12*, 514-521.

Cerdan, P.D., and Chory, J. (2003). Regulation of flowering time by light quality. Nature *423*, 881-885.

Chen, M., Galvao, R.M., Li, M., Burger, B., Bugea, J., Bolado, J., and Chory, J. (2010). Arabidopsis HEMERA/pTAC12 initiates photomorphogenesis by phytochromes. Cell *141*, 1230-1240.

Ciftci-Yilmaz, S., and Mittler, R. (2008). The zinc finger network of plants. Cellular and molecular life sciences : CMLS *65*, 1150-1160.

Collier, S., Pendle, A., Boudonck, K., van Rij, T., Dolan, L., and Shaw, P. (2006). A distant coilin homologue is required for the formation of cajal bodies in Arabidopsis. Molecular biology of the cell *17*, 2942-2951.

Corrales, A.R., Nebauer, S.G., Carrillo, L., Fernandez-Nohales, P., Marques, J., Renau-Morata, B., Granell, A., Pollmann, S., Vicente-Carbajosa, J., Molina, R.V.*, et al.* (2014). Characterization of tomato Cycling Dof Factors reveals conserved and new functions in the control of flowering time and abiotic stress responses. Journal of experimental botany *65*, 995-1012.

de Jong, R.N., Truffault, V., Diercks, T., Ab, E., Daniels, M.A., Kaptein, R., and Folkers, G.E. (2008). Structure and DNA binding of the human Rtf1 Plus3 domain. Structure *16*, 149-159.

Endo, M., Tanigawa, Y., Murakami, T., Araki, T., and Nagatani, A. (2013). PHYTOCHROME-DEPENDENT LATE-FLOWERING accelerates flowering through physical interactions with phytochrome B and CONSTANS. Proceedings of the National Academy of Sciences of the United States of America *110*, 18017-18022.

Feng, C.M., Qiu, Y., Van Buskirk, E.K., Yang, E.J., and Chen, M. (2014). Light-regulated gene repositioning in Arabidopsis. Nature communications *5*, 3027.

Guo, H., Yang, H., Mockler, T.C., and Lin, C. (1998). Regulation of flowering time by Arabidopsis photoreceptors. Science *279*, 1360-1363.

Hajdu, A., Adam, E., Sheerin, D.J., Dobos, O., Bernula, P., Hiltbrunner, A., Kozma-Bognar, L., and Nagy, F. (2015). High-level expression and phosphorylation of phytochrome B modulates flowering time in Arabidopsis. The Plant journal : for cell and molecular biology.

Hu, W., dePamphilis, C.W., and Ma, H. (2008). Phylogenetic analysis of the plant-specific zinc finger-homeobox and mini zinc finger gene families. Journal of integrative plant biology *50*, 1031-1045.

Hughes, R.M., Vrana, J.D., Song, J., and Tucker, C.L. (2012). Light-dependent, dark-promoted interaction between Arabidopsis cryptochrome 1 and phytochrome B proteins. The Journal of biological chemistry *287*, 22165-22172.

Jaillais, Y., Hothorn, M., Belkhadir, Y., Dabi, T., Nimchuk, Z.L., Meyerowitz, E.M., and Chory, J. (2011). Tyrosine phosphorylation controls brassinosteroid receptor activation by triggering membrane release of its kinase inhibitor. Genes & development *25*, 232-237.

Kaiserli, E., and Jenkins, G.I. (2007). UV-B promotes rapid nuclear translocation of the Arabidopsis UV-B specific signaling component UVR8 and activates its function in the nucleus. The Plant cell *19*, 2662-2673.

Kaiserli, E., Sullivan, S., Jones, M.A., Feeney, K.A., and Christie, J.M. (2009). Domain swapping to assess the mechanistic basis of Arabidopsis phototropin 1 receptor kinase activation and endocytosis by blue light. The Plant cell *21*, 3226-3244.

Kardailsky, I., Shukla, V.K., Ahn, J.H., Dagenais, N., Christensen, S.K., Nguyen, J.T., Chory, J., Harrison, M.J., and Weigel, D. (1999). Activation tagging of the floral inducer FT. Science *286*, 1962-1965.

Kircher, S., Gil, P., Kozma-Bognar, L., Fejes, E., Speth, V., Husselstein-Muller, T., Bauer, D., Adam, E., Schafer, E., and Nagy, F. (2002). Nucleocytoplasmic partitioning of the plant photoreceptors phytochrome A, B, C, D, and E is regulated differentially by light and exhibits a diurnal rhythm. The Plant cell *14*, 1541-1555.

Kircher, S., Kozma-Bognar, L., Kim, L., Adam, E., Harter, K., Schafer, E., and Nagy, F. (1999). Light quality-dependent nuclear import of the plant photoreceptors phytochrome A and B. The Plant cell *11*, 1445-1456.

Koroleva, O.A., Brown, J.W., and Shaw, P.J. (2009). Localization of eIF4A-III in the nucleolus and splicing speckles is an indicator of plant stress. Plant signaling & behavior *4*, 1148-1151.

Koroleva, O.A., Tomlinson, M., Parinyapong, P., Sakvarelidze, L., Leader, D., Shaw, P., and Doonan, J.H. (2004). CycD1, a putative G1 cyclin from Antirrhinum majus, accelerates the cell cycle in cultured tobacco BY-2 cells by enhancing both G1/S entry and progression through S and G2 phases. The Plant cell *16*, 2364-2379.

Lamond, A.I., and Spector, D.L. (2003). Nuclear speckles: a model for nuclear organelles. Nature reviews. Molecular cell biology *4*, 605-612.

Leivar, P., and Quail, P.H. (2011). PIFs: pivotal components in a cellular signaling hub. Trends in plant science *16*, 19-28.

Li, J., Jia, D., and Chen, X. (2001). HUA1, a regulator of stamen and carpel identities in Arabidopsis, codes for a nuclear RNA binding protein. The Plant cell *13*, 2269-2281.

Li, Q., Kim, Y., Namm, J., Kulkarni, A., Rosania, G.R., Ahn, Y.H., and Chang, Y.T. (2006). RNA-selective, live cell imaging probes for studying nuclear structure and function. Chemistry & biology *13*, 615-623.

Liu, Y., Liu, Q., Yan, Q., Shi, L., and Fang, Y. (2014). Nucleolus-tethering system (NoTS) reveals that assembly of photobodies follows a self-organization model. Molecular biology of the cell *25*, 1366-1373.

Loudet, O., Michael, T.P., Burger, B.T., Le Mette, C., Mockler, T.C., Weigel, D., and Chory, J. (2008). A zinc knuckle protein that negatively controls morning-specific growth in Arabidopsis thaliana. Proceedings of the National Academy of Sciences of the United States of America *105*, 17193-17198.

Mas, P., Devlin, P.F., Panda, S., and Kay, S.A. (2000). Functional interaction of phytochrome B and cryptochrome 2. Nature *408*, 207-211.

Matera, A.G., Izaguire-Sierra, M., Praveen, K., and Rajendra, T.K. (2009). Nuclear bodies: random aggregates of sticky proteins or crucibles of macromolecular assembly? Developmental cell *17*, 639-647.

Neff, M.M., and Chory, J. (1998). Genetic interactions between phytochrome A, phytochrome B, and cryptochrome 1 during Arabidopsis development. Plant physiology *118*, 27-35.

Nusinow, D.A., Helfer, A., Hamilton, E.E., King, J.J., Imaizumi, T., Schultz, T.F., Farre, E.M., and Kay, S.A. (2011). The ELF4-ELF3-LUX complex links the circadian clock to diurnal control of hypocotyl growth. Nature *475*, 398-402.

Papantonis, A., and Cook, P.R. (2013). Transcription factories: genome organization and gene regulation. Chemical reviews *113*, 8683-8705.

Qiu, Y., Li, M., Pasoreck, E.K., Long, L., Shi, Y., Galvao, R.M., Chou, C.L., Wang, H., Sun, A.Y., Zhang, Y.C.*, et al.* (2015). HEMERA Couples the Proteolysis and Transcriptional Activity of PHYTOCHROME INTERACTING FACTORs in Arabidopsis Photomorphogenesis. The Plant cell *27*, 1409-1427.

Rausenberger, J., Tscheuschler, A., Nordmeier, W., Wust, F., Timmer, J., Schafer, E., Fleck, C., and Hiltbrunner, A. (2011). Photoconversion and nuclear trafficking cycles determine phytochrome A's response profile to far-red light. Cell *146*, 813-825.

Sawa, M., Nusinow, D.A., Kay, S.A., and Imaizumi, T. (2007). FKF1 and GIGANTEA complex formation is required for day-length measurement in Arabidopsis. Science *318*, 261-265.

Sellaro, R., Hoecker, U., Yanovsky, M., Chory, J., and Casal, J.J. (2009). Synergism of red and blue light in the control of Arabidopsis gene expression and development. Current biology : CB *19*, 1216-1220.

Seo, H.S., Watanabe, E., Tokutomi, S., Nagatani, A., and Chua, N.H. (2004). Photoreceptor ubiquitination by COP1 E3 ligase desensitizes phytochrome A signaling. Genes & development *18*, 617-622.

Shikata, H., Hanada, K., Ushijima, T., Nakashima, M., Suzuki, Y., and Matsushita, T. (2014). Phytochrome controls alternative splicing to mediate light responses in Arabidopsis. Proceedings of the National Academy of Sciences of the United States of America *111*, 18781-18786.

Song, Y.H., Lee, I., Lee, S.Y., Imaizumi, T., and Hong, J.C. (2012a). CONSTANS and ASYMMETRIC LEAVES 1 complex is involved in the induction of FLOWERING LOCUS T in photoperiodic flowering in Arabidopsis. The Plant journal : for cell and molecular biology *69*, 332-342.

Song, Y.H., Smith, R.W., To, B.J., Millar, A.J., and Imaizumi, T. (2012b). FKF1 conveys timing information for CONSTANS stabilization in photoperiodic flowering. Science *336*, 1045-1049.

Sutherland, H., and Bickmore, W.A. (2009). Transcription factories: gene expression in unions? Nature reviews. Genetics *10*, 457-466.

Tan, Q.K., and Irish, V.F. (2006). The Arabidopsis zinc finger-homeodomain genes encode proteins with unique biochemical properties that are coordinately expressed during floral development. Plant physiology *140*, 1095-1108.

Tepperman, J.M., Zhu, T., Chang, H.S., Wang, X., and Quail, P.H. (2001). Multiple transcription-factor genes are early targets of phytochrome A signaling. Proceedings of the National Academy of Sciences of the United States of America *98*, 9437-9442.

Trupkin, S.A., Legris, M., Buchovsky, A.S., Tolava Rivero, M.B., and Casal, J.J. (2014). Phytochrome B Nuclear Bodies Respond to the Low Red to Far-Red Ratio and to the Reduced Irradiance of Canopy Shade in Arabidopsis. Plant physiology *165*, 1698-1708.

Valverde, F., Mouradov, A., Soppe, W., Ravenscroft, D., Samach, A., and Coupland, G. (2004). Photoreceptor regulation of CONSTANS protein in photoperiodic flowering. Science *303*, 1003-1006.

Van Buskirk, E.K., Decker, P.V., and Chen, M. (2012). Photobodies in light signaling. Plant physiology *158*, 52-60.

Van Buskirk, E.K., Reddy, A.K., Nagatani, A., and Chen, M. (2014). Photobody Localization of Phytochrome B Is Tightly Correlated with Prolonged and Light-Dependent Inhibition of Hypocotyl Elongation in the Dark. Plant physiology *165*, 595-607.

van Zanten, M., Tessadori, F., McLoughlin, F., Smith, R., Millenaar, F.F., van Driel, R., Voesenek, L.A., Peeters, A.J., and Fransz, P. (2010). Photoreceptors CRYTOCHROME2 and phytochrome B control chromatin compaction in Arabidopsis. Plant physiology *154*, 1686-1696.

van Zanten, M., Tessadori, F., Peeters, A.J., and Fransz, P. (2012). Shedding light on large-scale chromatin reorganization in Arabidopsis thaliana. Molecular plant *5*, 583-590.

Viczian, A., Adam, E., Wolf, I., Bindics, J., Kircher, S., Heijde, M., Ulm, R., Schafer, E., and Nagy, F. (2012). A short amino-terminal part of Arabidopsis phytochrome A induces constitutive photomorphogenic response. Molecular plant *5*, 629-641.

Wier, A.D., Mayekar, M.K., Heroux, A., Arndt, K.M., and VanDemark, A.P. (2013). Structural basis for Spt5-mediated recruitment of the Paf1 complex to chromatin. Proceedings of the National Academy of Sciences of the United States of America *110*, 17290-17295.

Wigge, P.A., Kim, M.C., Jaeger, K.E., Busch, W., Schmid, M., Lohmann, J.U., and Weigel, D. (2005). Integration of spatial and temporal information during floral induction in Arabidopsis. Science *309*, 1056-1059.

Yamaguchi, R., Nakamura, M., Mochizuki, N., Kay, S.A., and Nagatani, A. (1999). Light-dependent translocation of a phytochrome B-GFP fusion protein to the nucleus in transgenic Arabidopsis. The Journal of cell biology *145*, 437-445.

Yu, J.W., Rubio, V., Lee, N.Y., Bai, S., Lee, S.Y., Kim, S.S., Liu, L., Zhang, Y., Irigoyen, M.L., Sullivan, J.A.*, et al.* (2008). COP1 and ELF3 control circadian function and photoperiodic flowering by regulating GI stability. Molecular cell *32*, 617-630.

Zhang, B., Wang, L., Zeng, L., Zhang, C., and Ma, H. (2015). Arabidopsis TOE proteins convey a photoperiodic signal to antagonize CONSTANS and regulate flowering time. Genes & development *29*, 975-987.

FIGURE LEGENDS

Figure 1. Nuclear localization pattern of TZP.

(A) Representative images of etiolated plants expressing TZP-GFP irradiated with blue (10 μmol m^2 s^{-1}, red (10 μmol m^2 s^{-1}) or far-red light (10 μmol m^2 s^{-1}) for 4h prior to examination using confocal microscopy. Coilin-RFP was used as a control. A brief 10 s irradiation using the 633 nm laser was applied to samples mounted on a slide prior to confocal imaging. Scale bars: 20 μm.

(B) Western blot analysis TZP-GFP protein levels in response to light treatments used for imaging experiments. UGPase was used as a loading control.

(C) Diurnal regulation of TZP nuclear body formation monitored on plants entrained to a Light / Dark, Red light/Dark, or Blue light/Dark photoperiod (12h light / 12h dark). S before ZT stands for subjective dark. Data are represented as mean ± SEM. (n = 50 nuclei).

Figure 2. TZP is highly dynamic when localized in nuclear bodies.

FRAP measurements of TZP-GFP when localized in nuclear bodies (A), nucleoplasm (B), or whole nuclei (C) (ROI 1). Control non-bleached regions were monitored for loss of fluorescence during imaging (ROI 2). Scale bars: 20 μm.

Figure 3. TZP associates with phyB.

(A) Co-localization studies between TZP-mCherry and phyB-CFP, and TZP-mCherry and ELF3-YFP in N. *benthamiana* under white light (75 μmol m^2 s^{-1}). Scale bars: 20 μm.

(B) Yeast-two-hybrid analysis of GAL4DB-TZP and GAL4AD-PHYB apoprotein interaction on selective ($L^-W^-H^-$ 100mM 3AT), non-selective (L^-W^-) media and quantitative β-galactosidase assay using ONPG.

(C) Co-immunoprecipitation assay of TZP-GFP and phyB from Arabidopsis plants irradiated with 10 μmol m^2 s^{-1} of blue, red or far-red light at ZT0 for a period of 4 hours. Input controls showing TZP, phyB and control UGPase protein levels prior to the co-IP, and TZP after the co-IP (D) Confocal images of white light-grown transgenic Arabidopsis expressing TZP-GFP in WT*, phyA* and *phyB* mutant backgrounds. Scale bars: 20 μm.

Figure 4. TZP nuclear bodies correlate with transcription.

(A) Representative images of three independent experimental repeats showing TZP-YFP and phyB-CFP in seedlings treated with control DMSO or transcriptional inhibitors. Scale bars: 20 μm. A minimum of 30 nuclei were examined for each treatment.

(B) Investigation of co-localization between TZP-YFP and heterochromatin or RNA using DAPI or E144 markers respectively. Scale bars: 20 μm.

(C) Single-stranded and double-stranded deoxyribonucleic acid binding assay using lyophilized powder attached to cellulose from calf thymus DNA. Equal concentrations of in vitro transcribed and translated FLAG-tagged protein (TZP, TZP^{ZFPLUS}, TZP^{PLUS}, TZP^{Z1+2} or ATHB23) was added to the beads and washed. Association of test protein with ssDNA or dsDNA was detected by immunoblot using anti-FLAG antibody. The ZF-HD transcription factor ATHB23 was used as a positive control.

Figure 5. TZP accelerates flowering by regulating phyB-dependent *FT* expression.

(A) Phenotypic characterization of flowering time in of WT and *phyB* transgenic plants overexpressing TZP. Plants were grown under long day LD 16h light/ 8h dark photoperiodic conditions. Data are represented as mean ± SEM (n = 10 plants).

(B-C) qRT-PCR analysis of relative *FT* transcript levels normalized with housekeeping genes *IPP2* and *ISU1*. Plants were harvested 8h after light onset on day 12 under LD white light (50 μmol m^2 s^{-1}) or (B) on day 4 under LD white (50 μmol m^2 s^{-1}), red (10 μmol m^2 s^{-1}), or blue (10 μmol m^2 s^{-1}) light conditions. WT was used a reference. Data are represented as mean ± SEM (n = 3).

Figure 6. TZP associates with the promoter of *FT*.

(A) Schematic of the *FT* locus and seven amplicon locations used for the ChIP analyses. ChIP qPCR analysis of TZP WT association with different chromatin regions of the *FT* locus. No enrichment was observed for WT. A region of the *HY5* promoter was used as a negative control.

(B) ChIP qPCR analysis of TZP and deletion variants TZP^{Nt}, TZP^{ZFPLUS} shows that the full-length protein is required for association with FT^{pro}.

(C) qRT-PCR analysis of relative *FT* transcript levels in transgenic lines over-expressing TZP, TZP^{Nt} or TZP^{ZFPLUS}. WT was used a reference. Data are represented as mean ± SEM (n = 3).

(D) Relative enrichment of TZP WT and TZP *phyB* on *FT* locus (V).

(A-D) Plants were harvested 8h after light onset on day 12 under LD photoperiodic conditions. Data are representative of three independent biological replicates.

(E) Relative enrichment of TZP WT on *FT* locus (V) in plants exposed to either red or far-red light (10 μmol m^2 s^{-1}) at ZT0 for a period of 4 hours.

Figure 7. TZP accelerates flowering independent of cryptochromes.

(A) Phenotypic characterization of flowering time in *cry1cry2* transgenic plants overexpressing TZP. Plants were grown under long day (16h light/ 8h dark) photoperiodic conditions. Data are represented as mean ± SEM (n = 10 plants).

(B) qRT-PCR analysis of relative *FT* transcript levels normalized to *ISU1* and *IPP2*. Plants were harvested 8h after light onset on day 12 under LD photoperiodic conditions. *cry1cry2* was used as a reference. Data are represented as mean ± SEM (n = 3).

(C) Western blot analysis of TZP-GFP levels in WT, *phyB* and *cry1cry2* backgrounds.

(D) A model describing the role of TZP as a positive regulator of photoperiodic flowering by inducing the expression of *FT* and *CO*. During the day phyB recruits TZP in nuclear bodies to associate with the promoter of *FT* and *CO* and induce their expression independently, synergistically or additively to CO.

Figure 1

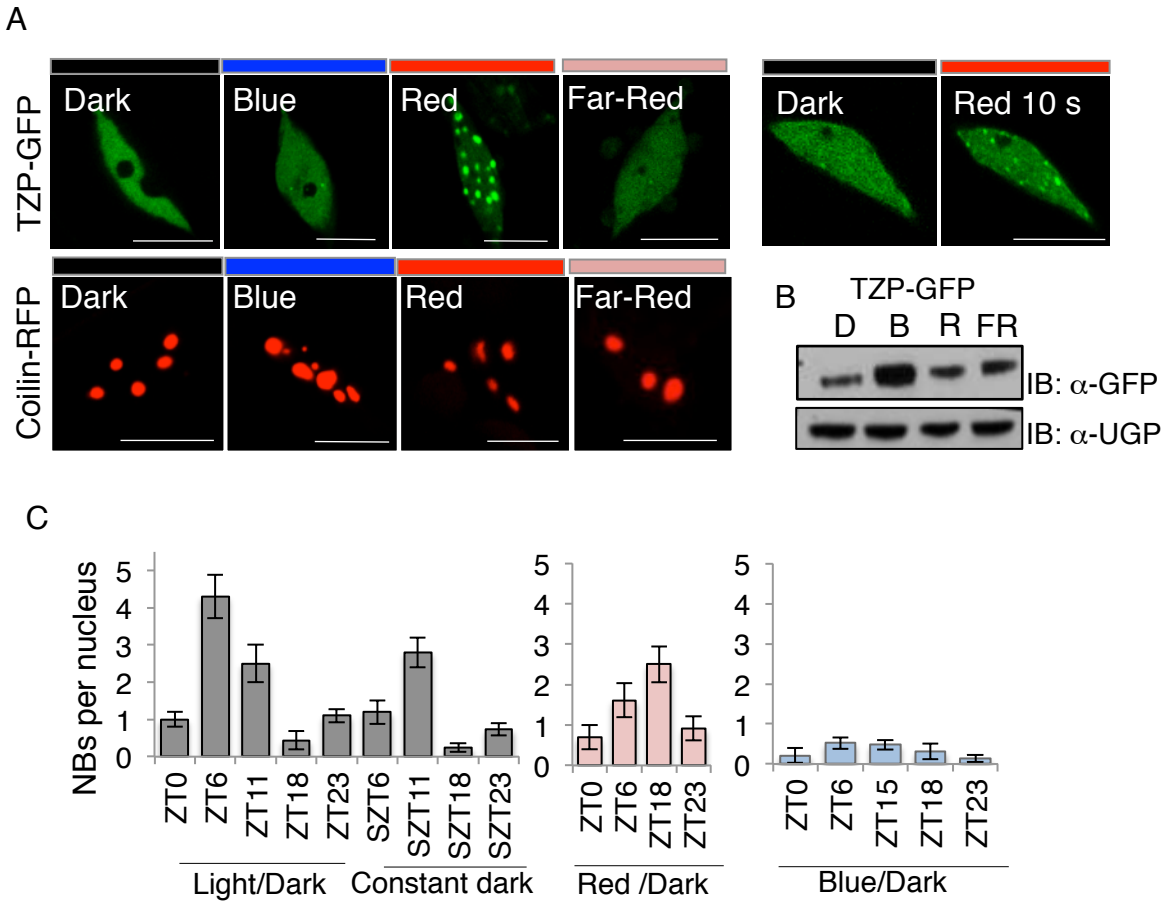
A
TZP-GFP
Dark
Blue
Red
Far-Red
Dark
Red 10 s
Coilin-RFP
Dark
Blue
Red
Far-Red
B
TZP-GFP
D B R FR
IB: α-GFP
IB: α-UGP
C
NBs per nucleus
0 1 2 3 4 5
ZT0 ZT6 ZT11 ZT18 ZT23 SZT6 SZT11 SZT18 SZT23
Light/Dark
Constant dark
ZT0 ZT6 ZT18 ZT23
Red /Dark
ZT0 ZT6 ZT15 ZT18 ZT23
Blue/Dark

Figure 2

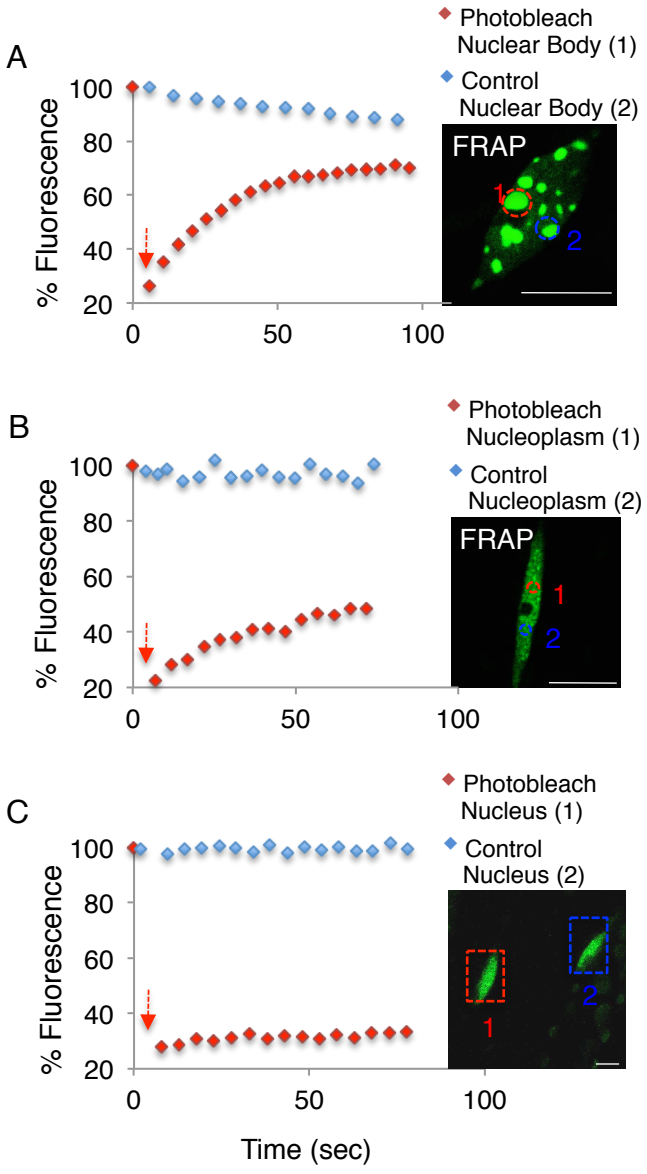
A
Photobleach
Nuclear Body (1)
Control
Nuclear Body (2)
FRAP
1
2
% Fluorescence
100
80
60
40
20
0
50
100
B
Photobleach
Nucleoplasm (1)
Control
Nucleoplasm (2)
FRAP
1
2
% Fluorescence
100
80
60
40
20
0
50
100
C
Photobleach
Nucleus (1)
Control
Nucleus (2)
1
2
% Fluorescence
100
80
60
40
20
0
50
100
Time (sec)

Figure 3

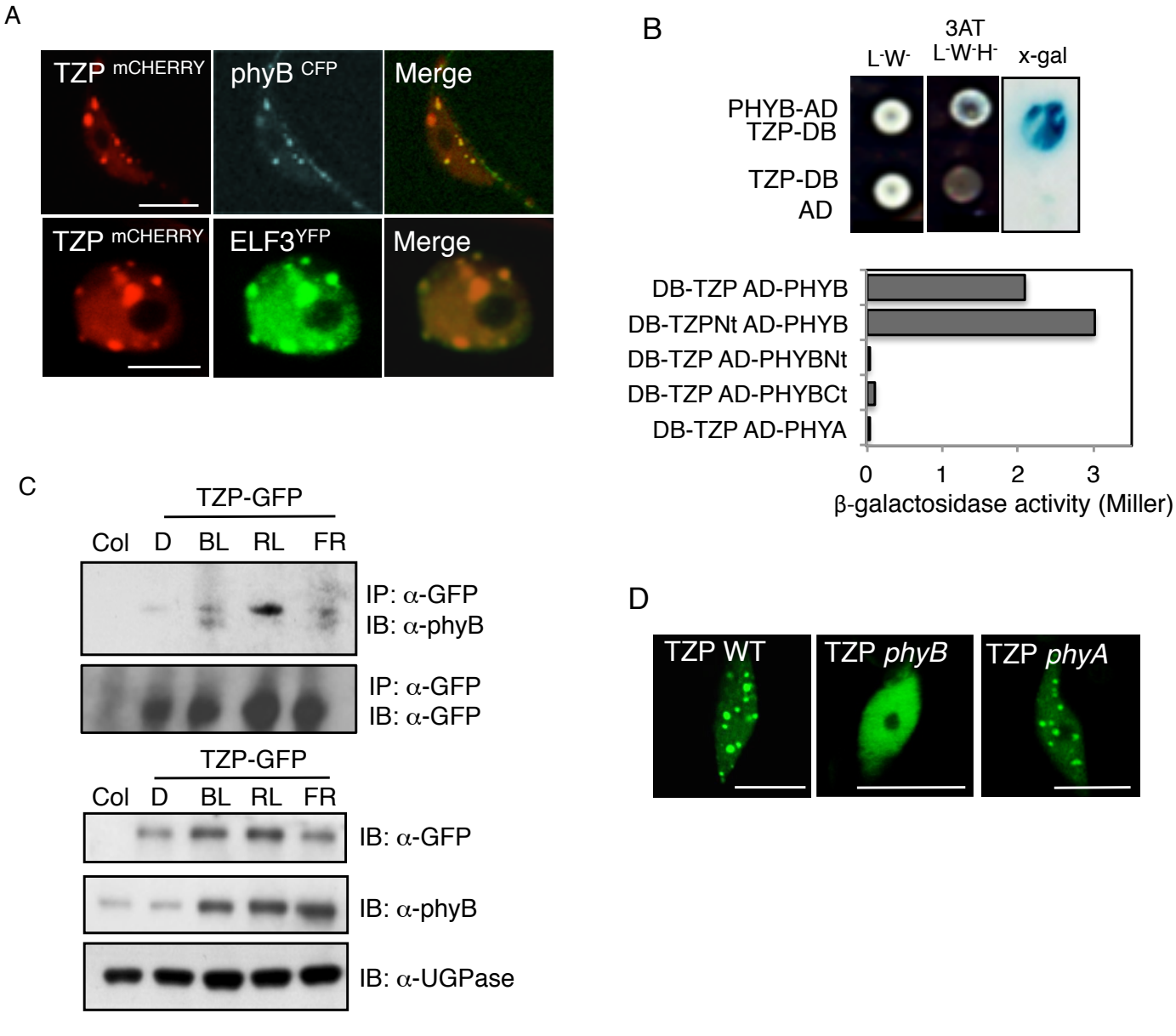
A
TZP mCHERRY
phyB CFP
Merge
TZP mCHERRY
ELF3YFP
Merge
B
3AT
L-W-
L-W-H-
x-gal
PHYB-AD
TZP-DB
TZP-DB
AD
DB-TZP AD-PHYB
DB-TZPNt AD-PHYB
DB-TZP AD-PHYBNt
DB-TZP AD-PHYBCt
DB-TZP AD-PHYA
0
1
2
3
β-galactosidase activity (Miller)
C
TZP-GFP
Col
D
BL
RL
FR
IP: α-GFP
IB: α-phyB
IP: α-GFP
IB: α-GFP
TZP-GFP
Col
D
BL
RL
FR
IB: α-GFP
IB: α-phyB
IB: α-UGPase
D
TZP WT
TZP phyB
TZP phyA

Figure 4

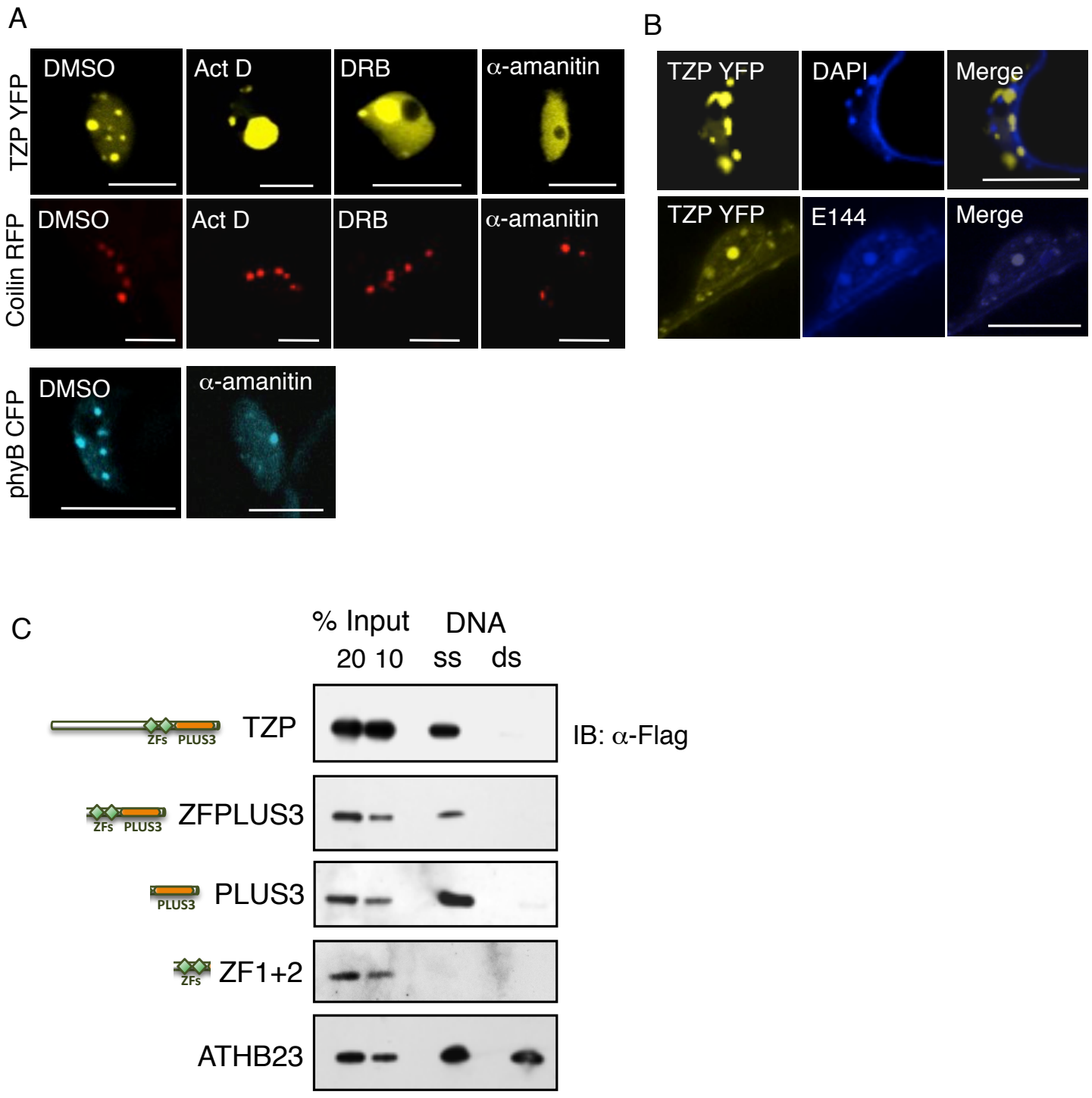
A
TZP YFP
DMSO
Act D
DRB
α-amanitin
Coilin RFP
DMSO
Act D
DRB
α-amanitin
phyB CFP
DMSO
α-amanitin
B
TZP YFP
DAPI
Merge
TZP YFP
E144
Merge
C
% Input
20 10
DNA
ss ds
ZFs PLUS3
TZP
IB: α-Flag
ZFs PLUS3
ZFPLUS3
PLUS3
PLUS3
ZFs
ZF1+2
ATHB23

Figure 5

A

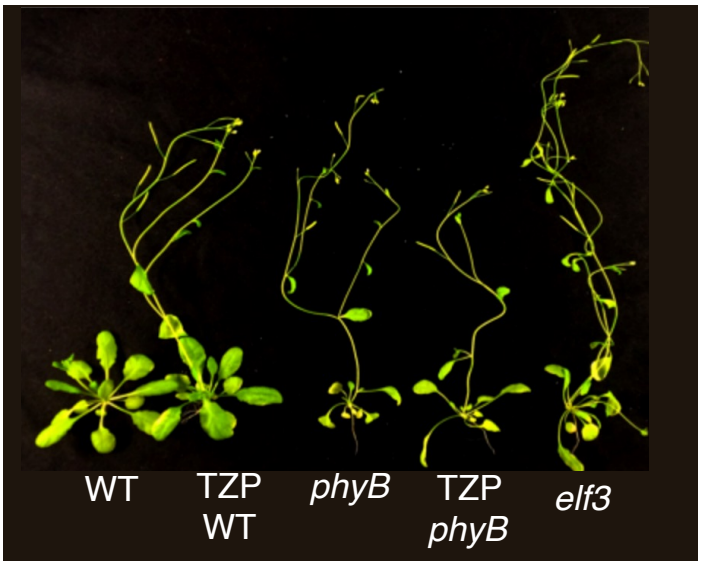
WT
TZP WT
phyB
TZP phyB
elf3

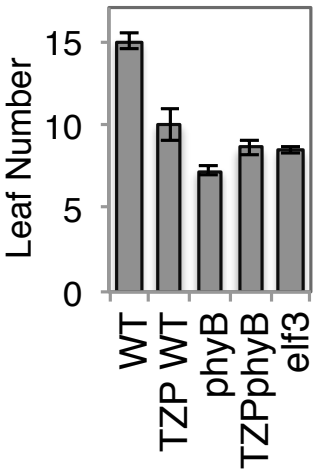
Leaf Number
0
5
10
15
WT
TZP WT
phyB
TZPphyB
elf3

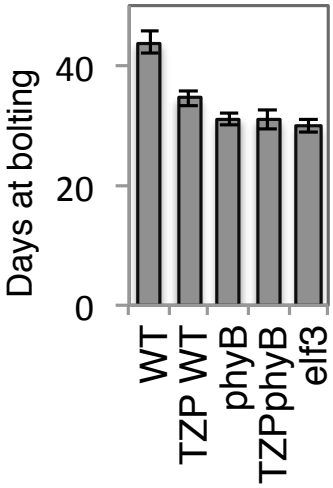
Days at bolting
0
20
40
WT
TZP WT
phyB
TZPphyB
elf3

B

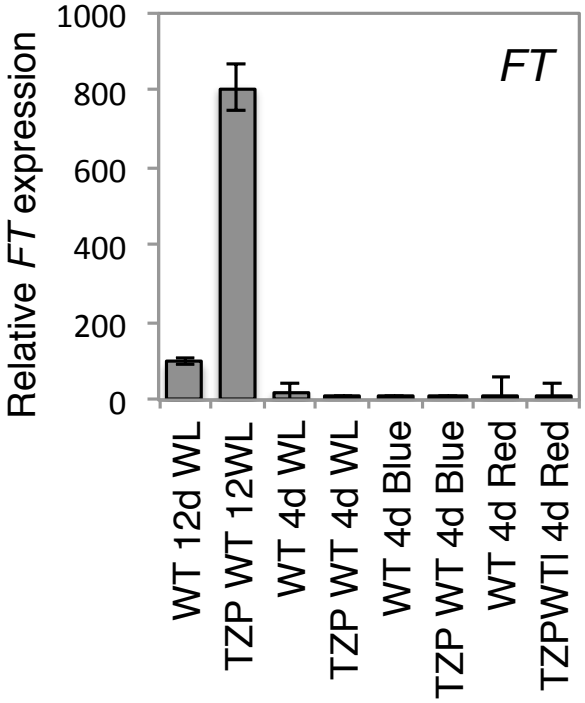
FT
Relative FT expression
0
200
400
600
800
1000
WT 12d WL
TZP WT 12WL
WT 4d WL
TZP WT 4d WL
WT 4d Blue
TZP WT 4d Blue
WT 4d Red
TZPWTl 4d Red

C

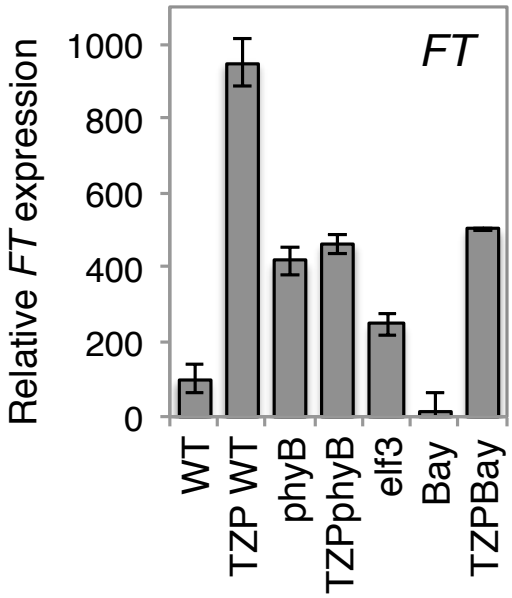
FT
Relative FT expression
0
200
400
600
800
1000
WT
TZP WT
phyB
TZPphyB
elf3
Bay
TZPBay

Figure 6

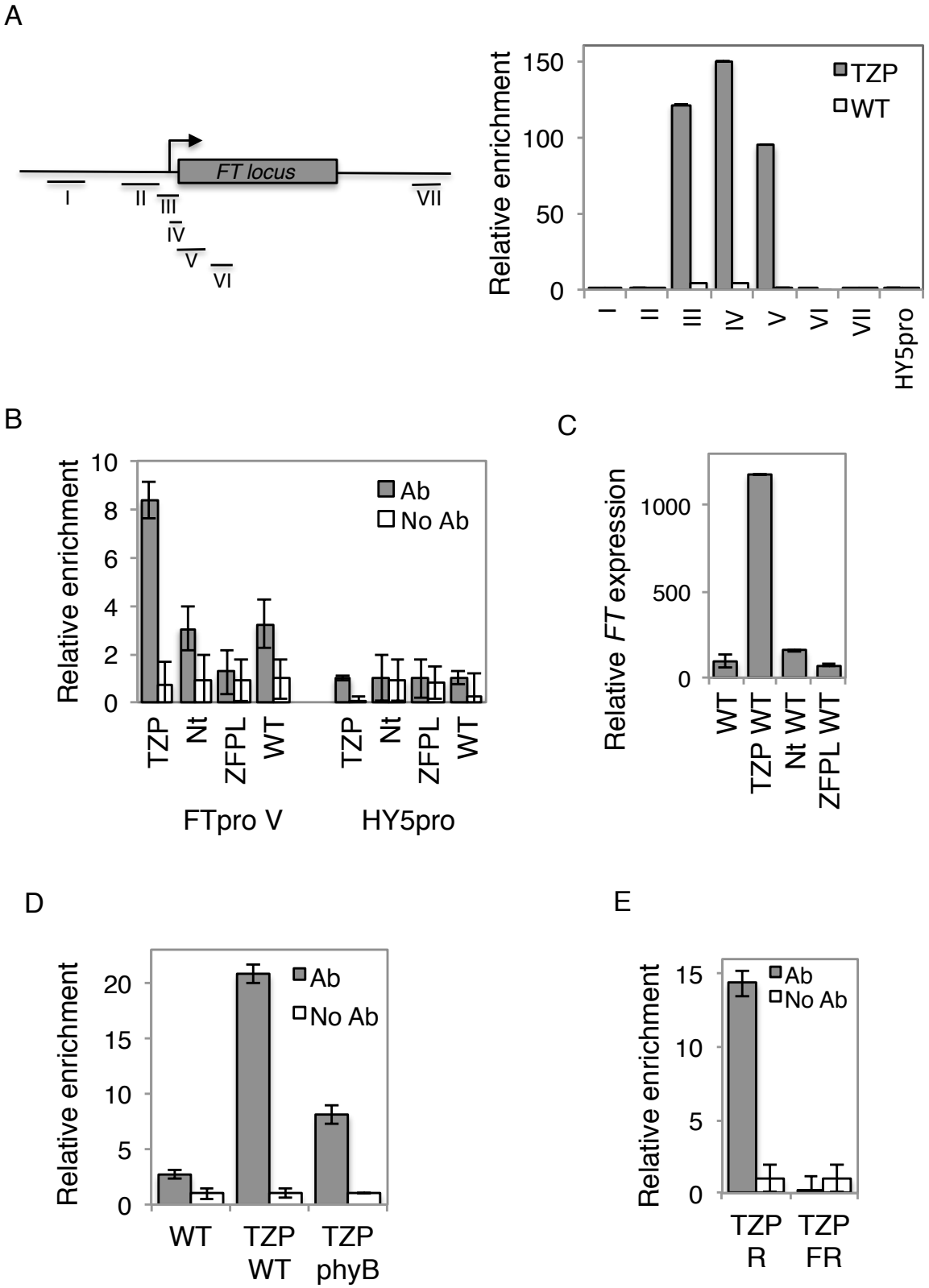
A
FT locus
I
II
III
IV
V
VI
VII
Relative enrichment
150
100
50
0
TZP
WT
I
II
III
IV
V
VI
VII
HY5pro
B
Relative enrichment
10
8
6
4
2
0
Ab
No Ab
TZP
Nt
ZFPL
WT
TZP
Nt
ZFPL
WT
FTpro V
HY5pro
C
Relative FT expression
1000
500
0
WT
TZP WT
Nt WT
ZFPL WT
D
Relative enrichment
20
15
10
5
0
Ab
No Ab
WT
TZP WT
TZP phyB
E
Relative enrichment
15
10
5
0
Ab
No Ab
TZP R
TZP FR

Figure 7

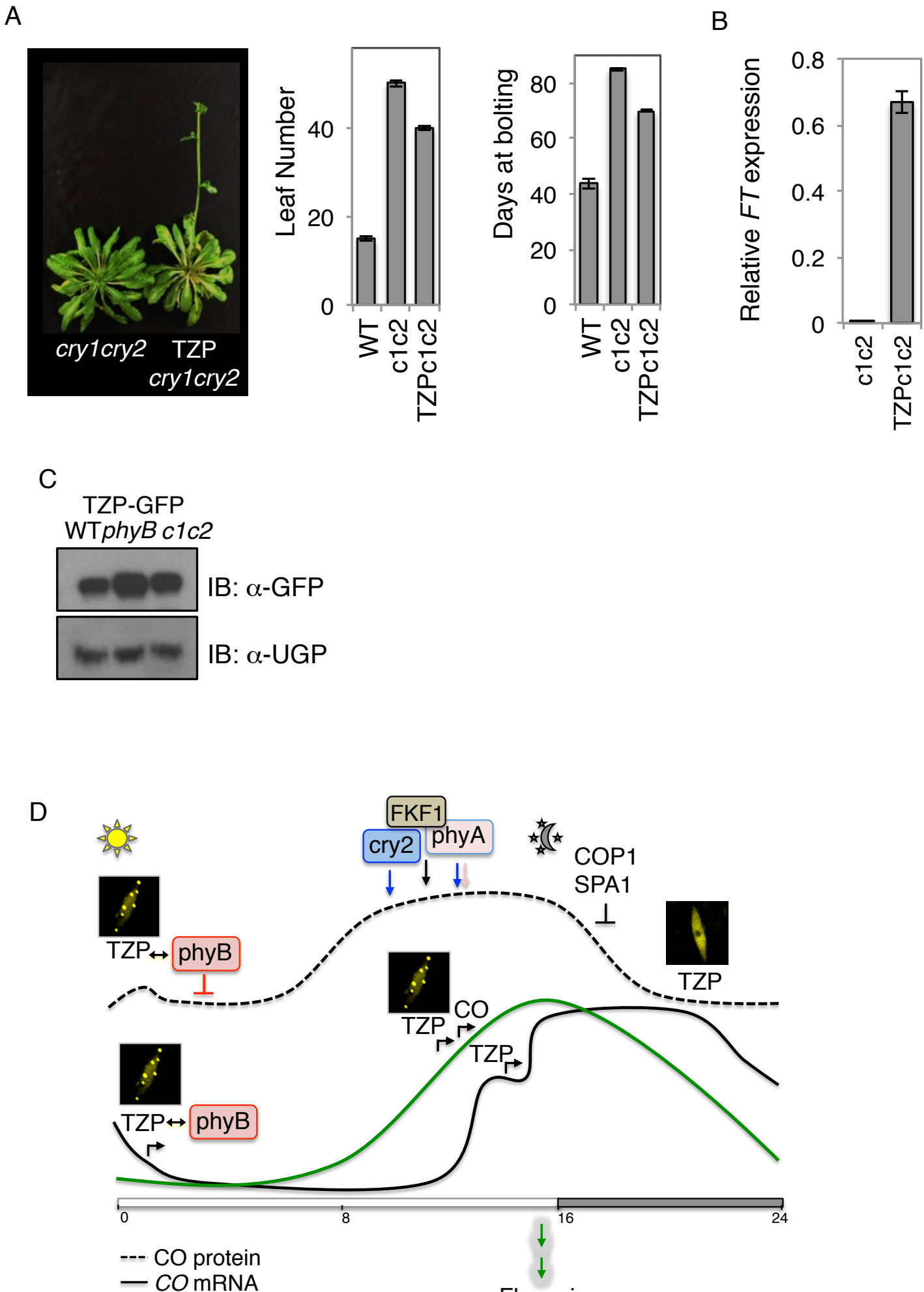
A
cry1cry2
TZP
cry1cry2
Leaf Number
0
20
40
WT
c1c2
TZPc1c2
Days at bolting
0
20
40
60
80
WT
c1c2
TZPc1c2
B
Relative FT expression
0
0.2
0.4
0.6
0.8
c1c2
TZPc1c2
C
TZP-GFP
WTphyB c1c2
IB: α-GFP
IB: α-UGP
D
FKF1
cry2
phyA
COP1
SPA1
TZP
phyB
TZP
CO
TZP
TZP
TZP
phyB
0
8
16
24
--- CO protein
— CO mRNA
— FT mRNA
Flowering

Figure S1 (Related to Figure 1)

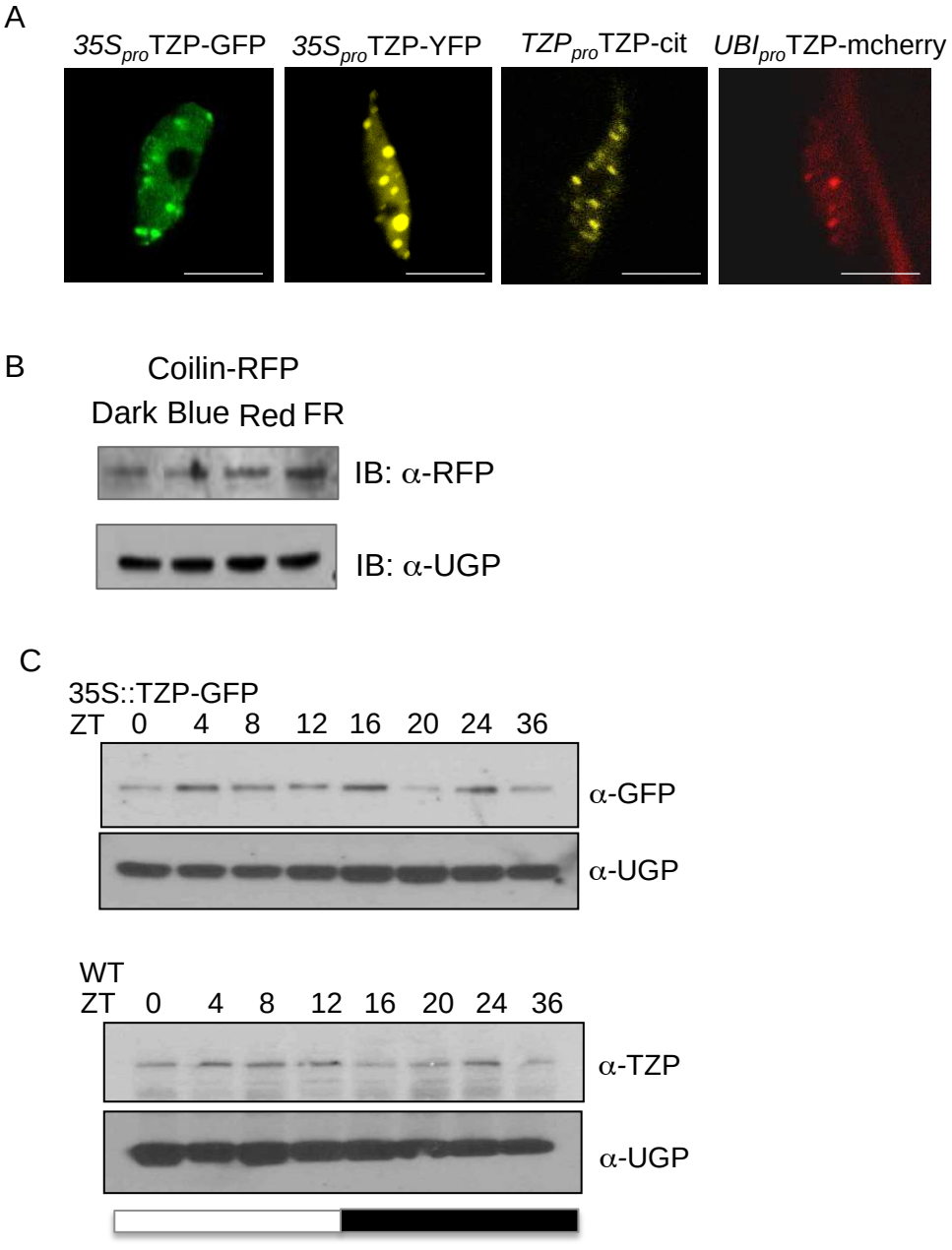

Figure S2 (Related to Figure 3)

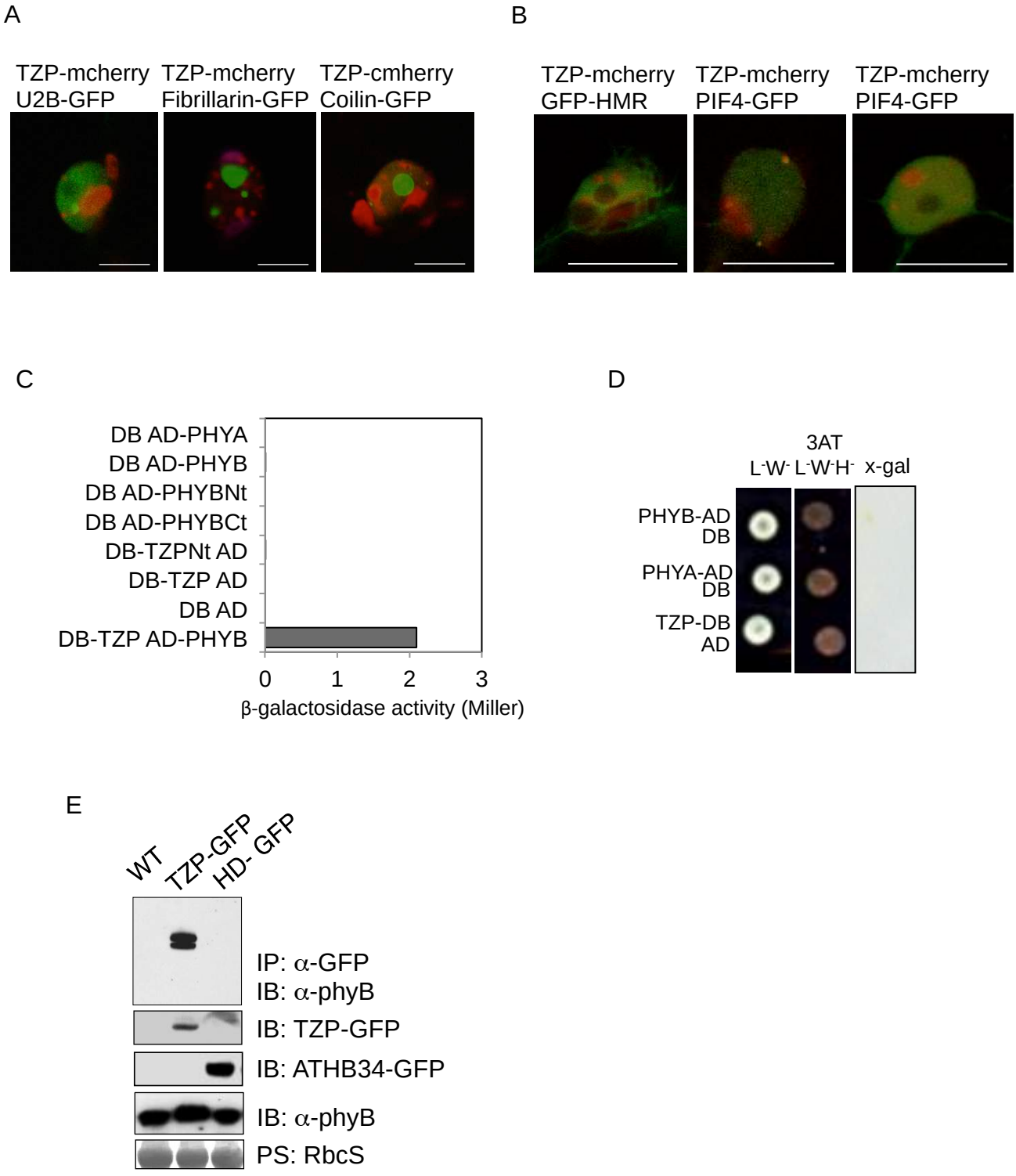

Figure S3 (Related to Figure 4)

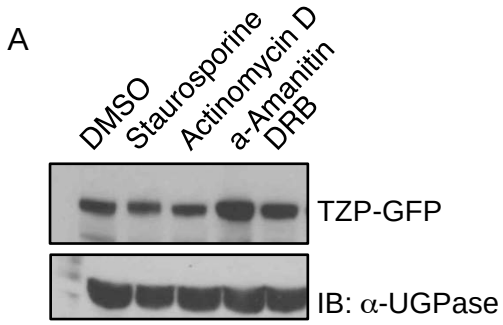

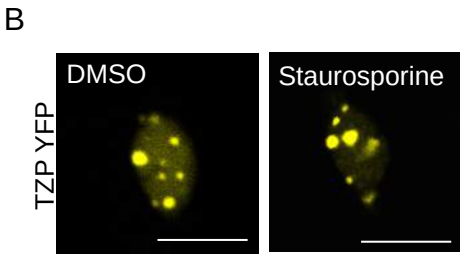

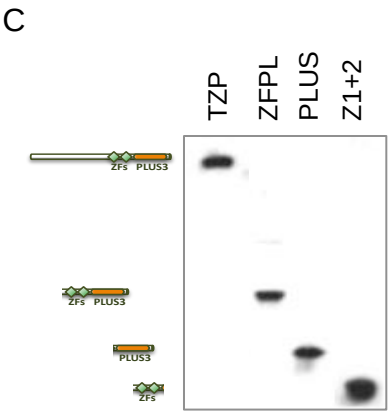

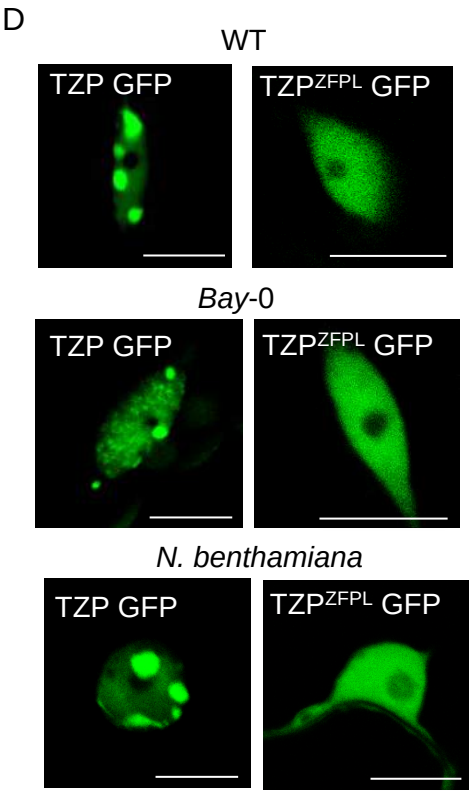

Figure S4 (Related to Figure 5)

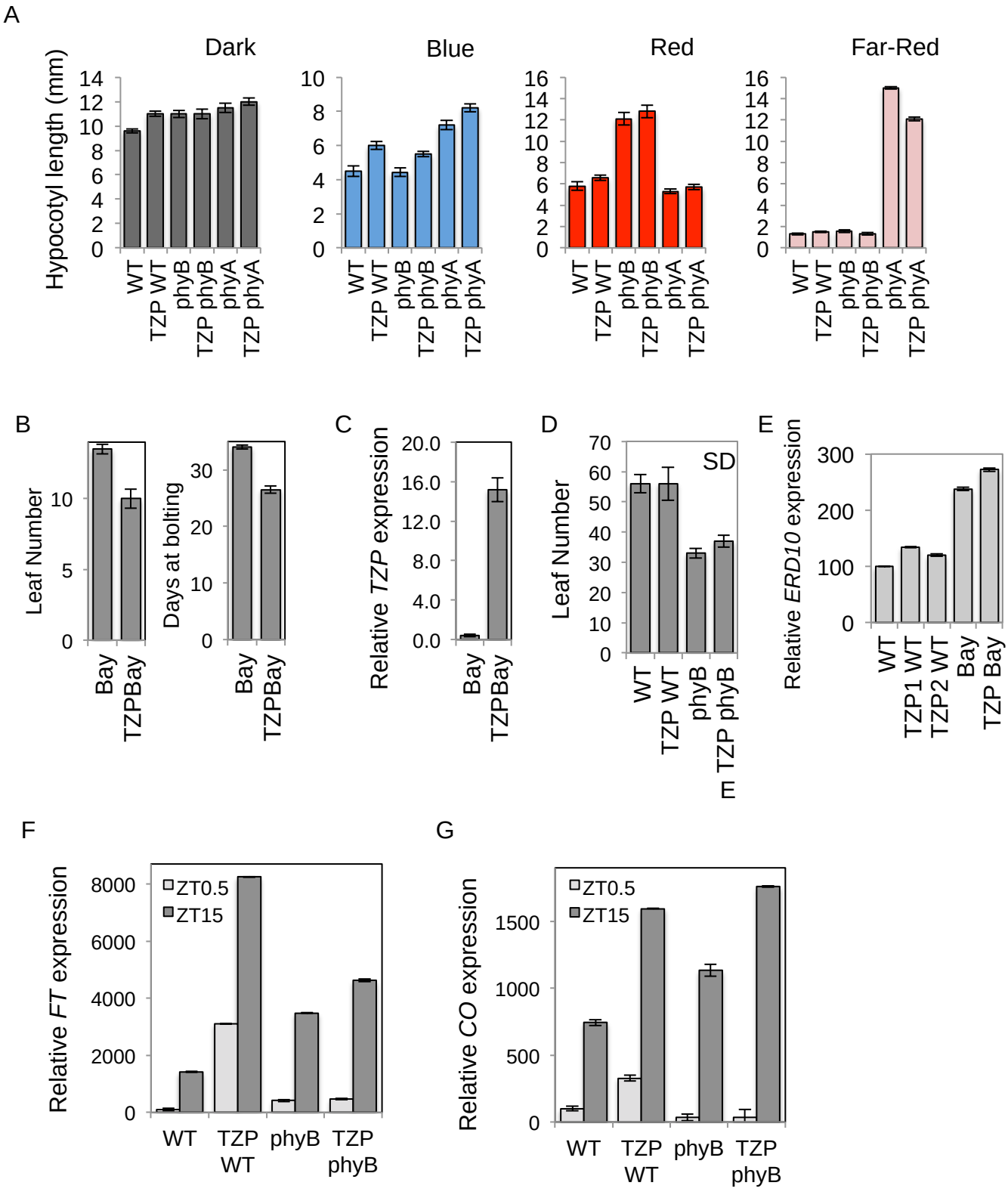

Figure S5 (Related to Figure 6)

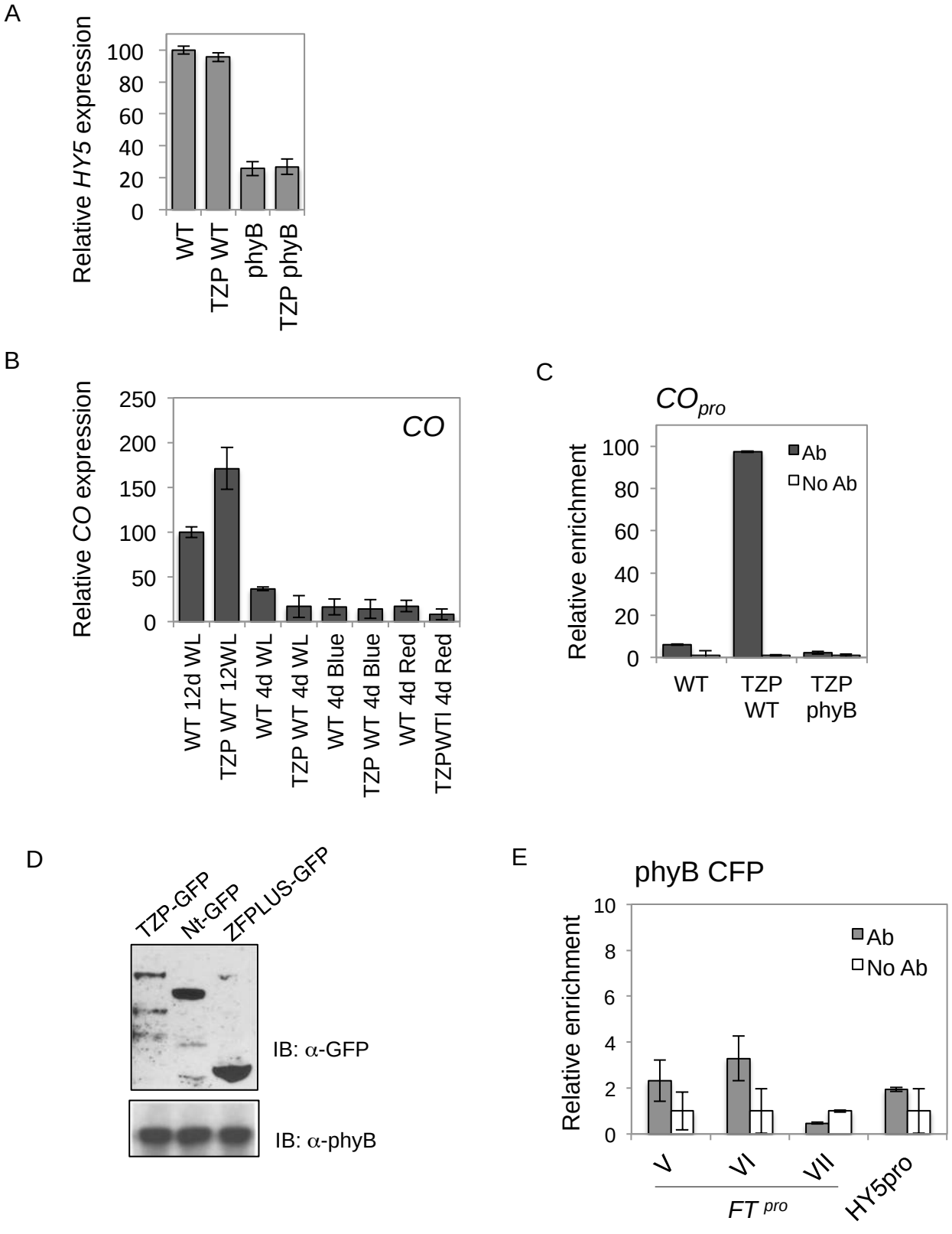

Figure S6 (Related to Figure 7)

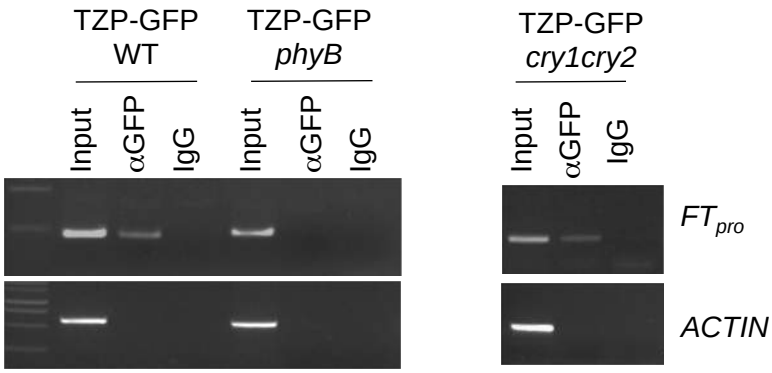

SUPPLEMENTAL MATERIAL

Figure S1. Localization and protein expression analysis of TZP. Related to Figure 1.

(A) Confocal image analysis of epidermal leaf tissue of light-grown transgenic Arabidopsis plants expressing *35S$_{pro}$*TZP-GFP, *35S$_{pro}$*TZP-YFP, *TZP$_{pro}$TZ*P-cit, *UBI$_{pro}$*TZP-mcherry. Scale bars: 20 mm. (B) Western blot analysis coilin-RFP protein levels in response to 4 hour light treatments used for imaging experiments (Figure 1A). UGPase was used as a loading control. (C) Western blot analysis of *35S$_{pro}$*TZP-GFP and native TZP protein levels during Light/Dark photoperiods (12L/12D). UGPase was used as a loading control.

Figure S2. Co-localization and protein interaction analysis of TZP. Related to Figure 3.

(A) Confocal images showing lack of co-localization between TZP-cherry with U2B-GFP, TZP-cherry with Fibrillarin-GFP and TZP-cherry with Coilin-RFP under white light (75 μmol m^2 s^{-1}). (B) Confocal image analysis of transient expressed N. *benthamiana* leaf tissue showing lack of co-localization between TZP-cherry and GFP-HMR and partial co-localisation with PIF4-GFP under white light (75 μmol m^2 s^{-1}). Scale bars: 20 mm. (C) Auto-activation assays for bait and prey constructs (DB-TZP, AD-PHYA, AD-PHYB) with the respective empty vectors using quantitative β-galactosiadase activity assay using ONPG as a substrate. (D) Auto-activation assays for bait and prey constructs (DB-TZP, AD-PHYA, AD-PHYB) with the respective

empty vectors on selective and non-selective media. (E) Co-immunoprecipitation assay of TZP-GFP and phyB from tissue extracted from white light grown Arabidopsis plants. Negative controls *WT* and ATHB34-GFP show no phyB immunoprecipitation. Input controls showing TZP, phyB, ATHB34-GFP and control RbcS prior to the co-IP.

Figure S3. Protein expression and localization studies of TZP in response to pharmacological treatments. Related to Figure 4.

(A) Western blot analysis of TZP-GFP protein levels after incubation with the inhibitors indicated in Figure 3A. UGPase was used as a loading control. (B) Confocal image analysis of TZP-YFP treated with control DMSO or staurosporine. Scale bars: 20 mm. (C) Western blot analysis of equal amounts of in vitro transcribed and translated TZP, TZP^{ZFPLUS}, TZP^{PLUS}, TZP $^{Z1+2}$ fused to a FLAG epitope tag protein. (D) Confocal image analysis of homozygous transgenic lines expressing TZP-GFP and TZP^{ZFPLUS}-GFP in WT, Bay-0 or transiently in N.*benthamiana* under white light (75 μmol m^2 s^{-1}). Scale bars: 20 μm.

Figure S4. TZP induces *FT* gene expression and flowering in Bay-0 ecotype. Related to Figure 5.

(A) Hypocotyl measurements of transgenic Arabidopsis lines overexpressing TZP in WT, *phyB* and *phyA* background and control WT plants grown for 5 days in darkness, red, blue or far-red light. Data are represented as mean ± SEM (n = 24 seedlings, n = 3 independent repeats). (B) Phenotypic characterization of flowering time in of Bay-0

transgenic plants overexpressing TZP. Plants were grown under long day (16h light/ 8h dark) photoperiodic conditions. Data are represented as mean ± SEM (n = 10 plants). (C) qRT-PCR analysis of relative *FT* transcript levels normalized with the housekeeping genes *ISU1 and IPP2*. Plants were harvested 8h after light onset on day 12 under LD. (D) Phenotypic characterization of flowering time of transgenic plants overexpressing TZP. Plants were grown under short day (8h light/ 16h dark) photoperiodic conditions. Data are represented as mean ± SEM (n = 10 plants).
(E) qRT-PCR analysis of relative *ERD10* transcript levels normalized with the housekeeping genes *ISU1.* Plants were harvested 8h after light onset on day 12 under LD photoperiod. (F-G) qRT-PCR analysis of relative *FT* (F) and *CO* (G) transcript levels normalized with the housekeeping genes *ISU1* and *IPP2.* Plants were grown under long day (16h light/ 8h dark) photoperiodic conditions and tissue was collected 0.5 h (ZT0.5) or 15 h (ZT15) after the onset of lights. Data are represented as mean ± SEM (n = 10 plants).

Figure S5. TZP regulates *CO* but not *HY5* gene expression. Related to Figure 6.
(A) qRT-PCR analysis of relative *HY5* transcript levels normalized with the housekeeping gene *ISU1*. Plants were harvested 8h after light onset on day 12 under LD. (A) qRT-PCR analysis of relative *CO* transcript levels normalized with the housekeeping gene *ISU1*. Plants were harvested 8h after light onset on day 12 under LD white light (50 μmol m^2 s^{-1}) or day 4 under LD white (50 μmol m^2 s^{-1}), red (10 μmol m^2 s^{-1}), or blue (10 μmol m^2 s^{-1}) light conditions. WT was used a reference. Data are represented as mean ± SEM (n = 3). (C) ChIP qPCR showing relative

enrichment of TZP WT and TZP *phyB* on *CO*. (D) Western blot analysis of protein levels of homozygous transgenic lines expressing TZP, TZP^{Nt} and TZP^{ZFPLUS} fused to GFP. phyB was used as a loading control. Tissue was collected 8h after light onset on day 12 under LD conditions. (E) Relative enrichment of phyB-CFP on *FT* and *HY5* loci. No significant enrichment was observed for phyB-CFP or WT. Plants were harvested 8h after light onset on day 12 under LD conditions. Data are representative of three independent biological replicates.

Figure S6. TZP associates with *FT* in the absence of cry1 and cry2. Related to Figure 7.

ChIP-PCR showing association of TZP with the promoter of *FT* when expressed WT and *c1c2,* but not in *phyB*. Plants were harvested 8h after light onset on day 12 under LD conditions. *ACTIN* was used as control locus. Data are representative of three independent biological replicates.

SUPPORTING METHODS

Plant material and growth conditions

Wild type (Col-0) and all Arabidopsis mutants (*phyB-9* (Reed et al., 1993) *cry1cry2* (*cry1-hy4-b104 cry2-1*; (Buchovsky et al., 2008)) and transgenic lines were in the Columbia (WT) background apart from Bay-0 and 35*S*TZP-GFP/Bay-0. Bay-0 derives from the Versailles resource center (http://dbsgap.versailles.inra.fr/vnat/) called ‘‘Bay-0[41AV]’’, progeny of CS954 (Loudet et al., 2008). *35S*phyB-CFP has been described previously (Nito et al., 2013). For subcellular localization analyses, ChIP

assays, transcript and proteins analyses, Arabidopsis seeds were surfaced sterilized and sown on 0.8% agar plates containing half-strength Linsmaier and Skoog salts in the absence of sucrose. Plates were stratified in the dark at 4°C for 48 hours and plants were grown as described in figure legends. Red, blue, far-red light treatments for hypocotyl measurements, confocal microscopy and protein analysis were performed in LED growth chambers (Percival Scientific) as described previously (Cole et al., 2011). Flowering time experiments were performed in Fitotron® growth rooms under the indicated photoperiod at 50 μmol m^2s^{-1} fluence rate white light. Plants were harvested 8h after light onset on day 12 under LD conditions for ChIP-PCR, and RT PCR experiments.

DNA constructs and generation of transgenic plants

The Gateway technology (Karimi et al., 2007) was used for the cloning of all constructs described on this study according the Life Technologies instructions. The *35S* and *UBI10* were described previously (Belkhadir et al., 2012; Jaillais et al., 2011a; Jaillais et al., 2011b). To generate gene fusions driven by the native TZP promoter (TZP), the –1548 to 0 genomic sequence upstream of the TZP coding sequence was PCR-amplified using the following primers: 5'CTTTTGACGACCACCTACAA 3' forward and 5' ACCTCCTGAAACCAATCAC 3' reverse. Primers used for the amplification of genes described in this study are listed in Supplemental Information. All plants were transformed and homozygous transgenic lines were selected as described previously (Kaiserli and Jenkins, 2007). A minimum of three independent homozygous transgenic lines were isolated and used for all

experimental procedures described in this study. Representative figures of three independent experimental repeats are shown in this study.

Yeast-two-hybrid assay

The ProQuest™ Two-Hybrid System (Invitrogen) was used to test direct interactions between TZP and phyB in yeast. cDNA coding for full-length TZP, TZP^{Nt} (1-601 aa), $TZP^{ZF\text{-}PLUS3}$ (602-831 aa) and TZP^{PLUS3} (695-831 aa) were cloned into the bait vector pDEST32 (GAL4DB). Full-length PHYA, PHYB, $PHYB^{Nt}$ (1-450 aa) and $PHYB^{Ct}$ (625-1152 aa) were cloned in the prey vector pDEST22 (GAL4AD). Deletions for PHYB were described previously (Oka et al., 2004). Protein expression of each construct was confirmed by western blot analysis. Transformation of MaV203 yeast cells and subsequent analysis of protein interactions on minimal (SD $Leu^{-}Trp^{-}$) and selective media (SD $Leu^{-}Trp^{-}His^{-}$, 100mM 3AT) was performed according to the manufacturer's instructions (Invitrogen). Quantitative measurements of β-galactosidase activity were assayed using the ONPG assay (Invitrogen).

Hypocotyl Measurements

Plates were rotated every day within each treatment chamber and were scanned in the end of the fifth day. Hypocotyl length was measured using NHI Image J. An average of 24 seedlings were measured for each treatment described.

Quantitative Real-Time PCR analysis

The following cycling conditions were used for quantitative PCR: 2 min at 95°C, 50 cycles of 3 s at 95°C, 30 s 59.5°C. Melt curve analysis from 60 - 90°C was performed to monitor the specificity of the amplification. The quantitative real-time PCR procedure used follows the MIQE (Minimum Information for Publication of Quantitative Real-Time PCR Experiments) guidelines (Bustin et al., 2009). The sample specific amplification efficiency was calculated according to the StepOne™ Software v2.2 (Life Technologies) using the slope of the regression line in the standard curve (standard dilution series: serial 4-fold dilutions, number of dilution points: 6). Using the standard curve the software interpolated the target quantities of each gene, which was later used to calculate the relative fold-differences. Normalization of the quantitative real-time PCR data was calculated by geometric averaging of the internal reference genes: *ISU1* and *IPP2* (Vandesompele et al., 2002). Primers used for qPCR have been published previously (*ACTIN:* (Kaiserli and Jenkins, 2007), *IPP2*: (Cole et al., 2011), *FT*: (Wang et al., 2009), TZP: (Loudet et al., 2008), *ERD10* (Corrales et al., 2014).

Unless otherwise stated, relative enrichment for ChIP-qPCR assays was calculated first by normalizing the amount of a target DNA fragment against a genomic fragment of a light regulated but non-TZP regulated gene, *HY5* or no antibody control and then by normalizing the value for WT plants as an internal control (Yan et al., 2014). Primers used for amplifying *FT* (Kumar et al., 2012; Lee et al., 2007), *CO* (Ito et al., 2012) *ACTIN* and *HY5* loci (Brown et al., 2005).

Western blot analysis and Antibodies

SDS-PAGE analysis was performed on 4-12% pre-cast, Bis-Tris gradient gels using MOPS buffer (Life Technologies). Western-blot analysis was performed using nitrocellulose membrane and the BIO-RAD protein transfer system.

The following antibodies were used: anti-GFP (ChIP grade Life Technologies, A-11122) anti-GFP (Roche), anti-DsRed (Clontech), anti-UGPase (Agrisera), anti-phyA (Nagatani lab, (Oka et al., 2004) anti-phyB (Nagatani Lab, (Oka et al., 2004), anti-mouse HRP (Bio-Rad), anti-rabbit HRP (Bio-Rad) were used at 1:5000 dilutions and anti-TZP (purified peptide antibody raised against the N-terminus of TZP was produced by GenScript) at 1:1000 dilution.

List of primers used:

qPCR

qISU1_for: GCCATCGCTTCTTCATCTGTTGC

qISU1_rev: TGGGAGAGAAAGATGCTTTG CG

qFT for CTAGCAACCCTCACCTCCGAGAATA

qFT rev CTGCCAAGCTGTCGAAACAATATAA

qCO for CCTCAGGGACTCACTACAACGAC

qCO rev GGTCAGGTTGTTGCTCTACTGTCC

qIPP2 for GTATGAGTTGCTTCTCCAGCAAAG

qIPP2 rev GAGGATGGCTGCAACAAGTGT

qHY5 for GGCTGAAGAGGTTGTTGAGG

qHY5 rev CAGCATTAGAACCACCACCA

qTZP for CCAAGACTTTCTTGAGGAGGAG

qTZP rev GCCGCTTGTTCTGGCACTT

ACTIN for CTTACAATTTCCCGCTCTGC

ACTIN rev GTTGGGATGAACCAGAAGGA

qERD10 for CGTTTGTGGCCAAGCACGAAG

qERD10 rev AGAGCTGTTGGATCGGTGGAGT

Cloning

TZP for: ATGGGAGATGGAGATGAGCA

TZP rev: AAAGCCTAACATTTTTCTCTGCTG

TZP PLUS for: ATGAGGGCGGTCTTTGATGCT

TZPNt rev: ATCCCTCTGTTCCTCCTCTGC

TZP ZF1 for: CTAATTTGTTTCTACTGCGG

TZP ZF2 rev CTA TGGTACGTCTGTGAAACCAC

TZPpro for CTTTTGACGACCACCTACAA

TZPpro rev ACCTCCTGAA ACCAATCAC

ELF3 for: ATGAAGAGAGGGAAAGATGAG

ELF3 rev: AGGCTTAGAGGAGTCATAT

ATHB34 for: ATGCTTGAAGTTAGATCAATGG

ATHB34 rev: CGACGAAGACGACGAGG

PHYB for: ATGGTTTCCGGAGTCGGGG

PHYB450 rev: CAGTGTCTGCGTTCTCAAAACGC

PHYB625 for: ATGAACTCTAAAGTTGTGGATGGTG

PHYA for: ATGTCAGGCTCTAGGCCGACT

PHYA rev: CTTGTTTGCTGCAGCGAGTT

U2B” for: ATGTTAACGGCAGATATACCAC

U2B” rev: TTTCTTGGCGAAAGAGATG

Fibrillarin for: ATGAGACCCCCAGTTACAGGAG

Fibrillarin rev: TGAGGCTGGGGTCTTTTGT

PIF4 for ATGGAACACCAAGGTTGGA

PIF4 rev GTGGTCCAAACGAGAACC

HMR for ATGGCGTCAATATCAACCAC

HMR rev AGGATCAGTCTCCTCTTCAAAGT

ChIP qPCR

FTpro I for AAGACGACAATGTGTGATGTACG

FTpro I rev TGATCTTGAACAAACAGGTGGT

FTpro II for TTGGCGGTACCCTACTTTTT

FTpro II rev TTTCGGATTTGCATTAACTCG

FTpro III for GTTATGATTTCACCGACCCGAGTT

FTpro III rev AGGTGGTTTCTCTGTGTTGATTGTTTC

FTpro IV for TTCATCTTTGAACTTAAGAAATGCTC

FTpro IV rev TTTTTATAAACAAGCGGCCATA

FTpro V for CAATCAACACAGAGAAACCAC

FTpro V rev AGGTCTTCTCCACCAATCTC

FTpro VI for GGTGGAGAAGACCTCAGGAA

FTpro VI rev GTGGGGCATTTTTAACCAAG

FTpro VII for GATCACTGATTCAACGCC

FTpro VII rev AGCATTAGACAGTAAGACCATC

COpro (−89 to +66) for CATGTAAGAGCCACTAACGC

COpro (−89 to +66) rev AACATAATAACTCAGATGTAGTAAG

HY5pro for TTGGTTTATGGCGGCTATAAA

HY5pro rev TGGCTACCGCCGTCAGAT

References:

Belkhadir, Y., Jaillais, Y., Epple, P., Balsemao-Pires, E., Dangl, J.L., and Chory, J. (2012). Brassinosteroids modulate the efficiency of plant immune responses to microbe-associated molecular patterns. Proceedings of the National Academy of Sciences of the United States of America *109*, 297-302.

Brown, B.A., Cloix, C., Jiang, G.H., Kaiserli, E., Herzyk, P., Kliebenstein, D.J., and Jenkins, G.I. (2005). A UV-B-specific signaling component orchestrates plant UV protection. Proceedings of the National Academy of Sciences of the United States of America *102*, 18225-18230.

Buchovsky, A.S., Strasser, B., Cerdan, P.D., and Casal, J.J. (2008). Suppression of pleiotropic effects of functional cryptochrome genes by Terminal Flower 1. Genetics *180*, 1467-1474.

Bustin, S.A., Benes, V., Garson, J.A., Hellemans, J., Huggett, J., Kubista, M., Mueller, R., Nolan, T., Pfaffl, M.W., Shipley, G.L.*, et al.* (2009). The MIQE guidelines: minimum information for publication of quantitative real-time PCR experiments. Clinical chemistry *55*, 611-622.

Cole, B., Kay, S.A., and Chory, J. (2011). Automated analysis of hypocotyl growth dynamics during shade avoidance in Arabidopsis. The Plant journal : for cell and molecular biology *65*, 991-1000.

Corrales, A.R., Nebauer, S.G., Carrillo, L., Fernandez-Nohales, P., Marques, J., Renau-Morata, B., Granell, A., Pollmann, S., Vicente-Carbajosa, J., Molina, R.V.*, et al.* (2014). Characterization of tomato Cycling Dof Factors reveals conserved and new functions in the control of flowering time and abiotic stress responses. Journal of experimental botany *65*, 995-1012.

Ito, S., Song, Y.H., Josephson-Day, A.R., Miller, R.J., Breton, G., Olmstead, R.G., and Imaizumi, T. (2012). FLOWERING BHLH transcriptional activators control expression of the photoperiodic flowering regulator CONSTANS in Arabidopsis. Proceedings of the National Academy of Sciences of the United States of America *109*, 3582-3587.

Jaillais, Y., Belkhadir, Y., Balsemao-Pires, E., Dangl, J.L., and Chory, J. (2011a). Extracellular leucine-rich repeats as a platform for receptor/coreceptor complex formation. Proceedings of the National Academy of Sciences of the United States of America *108*, 8503-8507.

Jaillais, Y., Hothorn, M., Belkhadir, Y., Dabi, T., Nimchuk, Z.L., Meyerowitz, E.M., and Chory, J. (2011b). Tyrosine phosphorylation controls brassinosteroid receptor activation by triggering membrane release of its kinase inhibitor. Genes & development *25*, 232-237.

Kaiserli, E., and Jenkins, G.I. (2007). UV-B promotes rapid nuclear translocation of the Arabidopsis UV-B specific signaling component UVR8 and activates its function in the nucleus. The Plant cell *19*, 2662-2673.

Karimi, M., Depicker, A., and Hilson, P. (2007). Recombinational cloning with plant gateway vectors. Plant physiology *145*, 1144-1154.

Kumar, S.V., Lucyshyn, D., Jaeger, K.E., Alos, E., Alvey, E., Harberd, N.P., and Wigge, P.A. (2012). Transcription factor PIF4 controls the thermosensory activation of flowering. Nature *484*, 242-245.

Lee, J.H., Yoo, S.J., Park, S.H., Hwang, I., Lee, J.S., and Ahn, J.H. (2007). Role of SVP in the control of flowering time by ambient temperature in Arabidopsis. Genes & development *21*, 397-402.

Loudet, O., Michael, T.P., Burger, B.T., Le Mette, C., Mockler, T.C., Weigel, D., and Chory, J. (2008). A zinc knuckle protein that negatively controls morning-specific growth in Arabidopsis thaliana. Proceedings of the National Academy of Sciences of the United States of America *105*, 17193-17198.

Nito, K., Wong, C.C., Yates, J.R., 3rd, and Chory, J. (2013). Tyrosine phosphorylation regulates the activity of phytochrome photoreceptors. Cell reports *3*, 1970-1979.

Oka, Y., Matsushita, T., Mochizuki, N., Suzuki, T., Tokutomi, S., and Nagatani, A. (2004). Functional analysis of a 450-amino acid N-terminal fragment of phytochrome B in Arabidopsis. The Plant cell *16*, 2104-2116.

Reed, J.W., Nagpal, P., Poole, D.S., Furuya, M., and Chory, J. (1993). Mutations in the gene for the red/far-red light receptor phytochrome B alter cell elongation and physiological responses throughout Arabidopsis development. The Plant cell *5*, 147-157.

Vandesompele, J., De Preter, K., Pattyn, F., Poppe, B., Van Roy, N., De Paepe, A., and Speleman, F. (2002). Accurate normalization of real-time quantitative RT-PCR data by geometric averaging of multiple internal control genes. Genome biology *3*, RESEARCH0034.

Wang, J.W., Czech, B., and Weigel, D. (2009). miR156-regulated SPL transcription factors define an endogenous flowering pathway in Arabidopsis thaliana. Cell *138*, 738-749.

Yan, Y., Shen, L., Chen, Y., Bao, S., Thong, Z., and Yu, H. (2014). A MYB-domain protein EFM mediates flowering responses to environmental cues in Arabidopsis. Developmental cell *30*, 437-448.